Molecular Therapy
Original Article

Preclinical Evaluation of Allogeneic CAR T Cells Targeting BCMA for the Treatment of Multiple Myeloma

Cesar Sommer,[1,5] Bijan Boldajipour,[2,5] Tracy C. Kuo,[2] Trevor Bentley,[1] Janette Sutton,[1] Amy Chen,[2] Tao Geng,[2] Holly Dong,[2] Roman Galetto,[3] Julien Valton,[4] Thomas Pertel,[1] Alexandre Juillerat,[4] Annabelle Gariboldi,[3] Edward Pascua,[2] Colleen Brown,[2] Sherman M. Chin,[2] Tao Sai,[2] Yajin Ni,[1] Philippe Duchateau,[3] Julianne Smith,[4] Arvind Rajpal,[2] Thomas Van Blarcom,[1] Javier Chaparro-Riggers,[2] and Barbra J. Sasu[1]

[1]Allogene Therapeutics, Inc., 210 E. Grand Avenue, South San Francisco, CA 94080, USA; [2]Pfizer Cancer Immunology Discovery, Pfizer Worldwide Research and Development, 230 E. Grand Avenue, South San Francisco, CA 94080, USA; [3]Cellectis SA, 8 rue de la Croix Jarry, 75013 Paris, France; [4]Cellectis, Inc., 430 East 29th Street, New York, NY 10016, USA

Clinical success of autologous CD19-directed chimeric antigen receptor T cells (CAR Ts) in acute lymphoblastic leukemia and non-Hodgkin lymphoma suggests that CAR Ts may be a promising therapy for hematological malignancies, including multiple myeloma. However, autologous CAR T therapies have limitations that may impact clinical use, including lengthy vein-to-vein time and manufacturing constraints. Allogeneic CAR T (AlloCAR T) therapies may overcome these innate limitations of autologous CAR T therapies. Unlike autologous cell therapies, AlloCAR T therapies employ healthy donor T cells that are isolated in a manufacturing facility, engineered to express CARs with specificity for a tumor-associated antigen, and modified using gene-editing technology to limit T cell receptor (TCR)-mediated immune responses. Here, transcription activator-like effector nuclease (TALEN) gene editing of B cell maturation antigen (BCMA) CAR Ts was used to confer lymphodepletion resistance and reduced graft-versus-host disease (GvHD) potential. The safety profile of allogeneic BCMA CAR Ts was further enhanced by incorporating a CD20 mimotope-based intra-CAR off switch enabling effective CAR T elimination in the presence of rituximab. Allogeneic BCMA CAR Ts induced sustained antitumor responses in mice supplemented with human cytokines, and, most importantly, maintained their phenotype and potency after scale-up manufacturing. This novel off-the-shelf allogeneic BCMA CAR T product is a promising candidate for clinical evaluation.

INTRODUCTION

Chimeric antigen receptor T cells (CAR Ts) have shown efficacy in hematological cancers, and two autologous CD19-targeted CAR T products have recently been approved by the Food and Drug Administration (FDA) for the treatment of B cell malignancies.[1,2] Patient age,[3–5] the number of prior lines of treatment,[6] and the disease itself[7,8] may limit the number and quality of patient-derived T cells, potentially influencing the potency and variability of the CAR T products. Furthermore, the logistics of clinical manufacturing using patient-derived T cells limits the accessibility of these therapies. An allogeneic CAR T approach has the potential to circumvent all these challenges by using healthy donor-derived T cells to produce CAR Ts that can be available as an off-the-shelf product.[9–12] One manufacturing run can create allogeneic CAR T (AlloCAR T) product for use in multiple patients and be stored off-the-shelf for on-demand treatment. CD19-targeted allogeneic CAR T therapies have produced promising results in patients with acute lymphoblastic leukemia (ALL),[13,14] and they are currently in clinical trials in Europe and the United States.

Multiple myeloma is a B cell malignancy that affects an elderly population with a median age of approximately 70 years.[15] Despite the development of numerous treatments, including chemotherapy, proteasome inhibitors, immunomodulators, depleting antibodies, and autologous stem cell transplantation, the disease is incurable and most patients eventually relapse.[16] B cell maturation antigen (BCMA) is a pro-survival tumor necrosis factor (TNF) receptor expressed in mature B cells and plasma cells,[17,18] and it is expressed on multiple myeloma cells at all stages of disease.[19,20] Therapies targeting BCMA have shown promise in clinical and preclinical studies,[19–23] and multiple groups are investigating the use of autologous CAR Ts for the treatment of BCMA-expressing hematological malignancies.[24–30]

Received 29 November 2018; accepted 2 April 2019;
https://doi.org/10.1016/j.ymthe.2019.04.001.

[5]These authors contributed equally to this work.

Correspondence: Cesar Sommer, Allogene Therapeutics, Inc., 210 E. Grand Avenue, South San Francisco, CA 94080, USA.
E-mail: cesar.sommer@allogene.com
Correspondence: Barbra J. Sasu, Allogene Therapeutics, Inc., 210 E. Grand Avenue, South San Francisco, CA 94080, USA.
E-mail: barbra.sasu@allogene.com

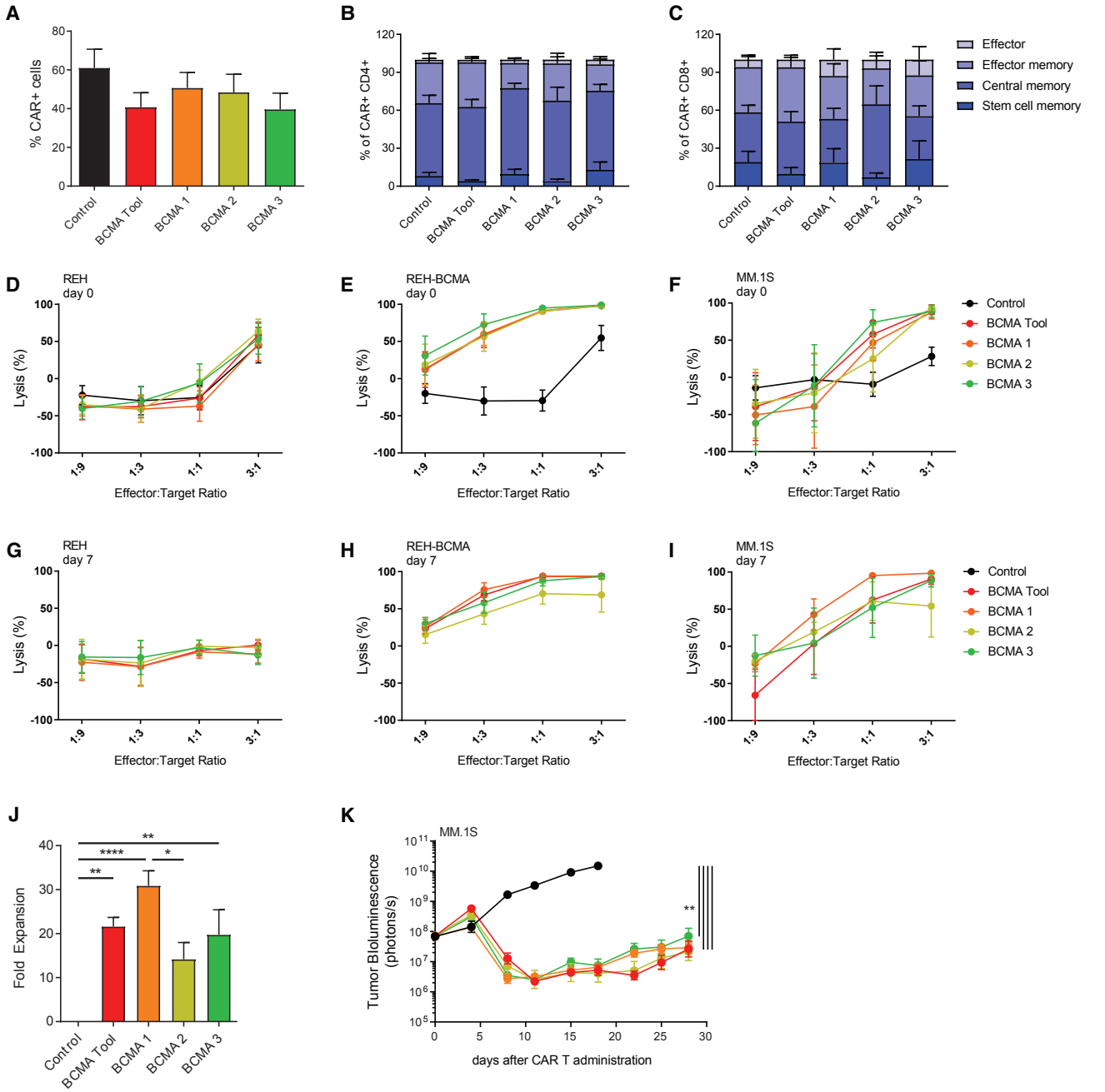

Figure 1. BCMA CAR Ts Show High Proliferative Potential and Potent Antitumor Activity

(A) All BCMA CAR constructs demonstrated similar transduction efficiencies, as detected by soluble BCMA staining using flow cytometry at day 14 of expansion (n = 5 donors). (B and C) BCMA CAR T candidates showed similar distribution of T cell subsets within the $CD4^+$ (B) and $CD8^+$ (C) cell populations. CAR Ts were analyzed using flow cytometry 14 days after activation, and phenotypes were assigned according to CD62L and CD45RO expression within the CAR^+ cell population as follows: stem cell memory ($CD45RO^-/CD62L^+$), central memory ($CD45RO^+/CD62L^+$), effector memory ($CD45RO^+/CD62L^-$), effector cells ($CD45RO^-/CD62L^-$) (n = 4 donors). (D–F) BCMA CAR T candidates showed similar cytotoxicity against BCMA-expressing target cells. CAR Ts were cultured with luciferase-expressing BCMA-negative REH cells (D), REH cells overexpressing BCMA (E), or MM.1S cells (F). Target cell luminescence was assessed after 24 h (n = 5 donors). (G–I) BCMA CAR Ts maintained cytotoxicity after repeated exposure to target cells. CAR Ts were tested similarly to (D)–(F), after 7 days and 3 rounds of co-culture with BCMA-expressing target cells (n = 5 donors). (J) BCMA 1 showed superior expansion potential in response to target cell exposure. CAR Ts were expanded on BCMA-expressing target cells 3 times within 7 days and quantified by

(legend continued on next page)

In this report, fully human CARs with a high affinity to BCMA were profiled for their ability to redirect T cell effector function against multiple myeloma cell lines using *in vitro* and *in vivo* models. A lead CAR was chosen for further modification to incorporate an intra-CAR off switch inducible by rituximab that showed no impact on CAR function and mediated effective CAR T elimination *in vitro* and *in vivo*. Engineering of T cells derived from healthy donors using transcription activator-like effector nucleases (TALENs) resulted in BCMA CAR Ts with reduced potential for graft-versus-host disease and resistant to a lymphodepleting anti-CD52 antibody that preserved their potency after scale-up manufacturing. Consistent with a role of homeostatic cytokines in maintaining T cell proliferation, adoptive transfer of BCMA CAR Ts into NOD.Cg-*Prkdc*^{scid} *Il2rg*^{tm1Wjl}/SzJ (NSG) mice producing human interleukin (IL)-7 and IL-15 at physiological levels dramatically improved their persistence and long-term antitumor activity. Taken together, these findings support further development of allogeneic BCMA CAR Ts as a novel treatment for multiple myeloma.

RESULTS

Generation of BCMA CAR T Candidates

Fully human, phage display-derived anti-BCMA antibodies had previously been tested for their ability to target BCMA as CD3-bispecific constructs (unpublished data). These antibodies bound to overlapping epitopes on BCMA and covered a range of affinities (0.038–5.57 nM; Table S1). Three single-chain variable fragments (scFvs), denoted as BCMA 1, 2, and 3, were initially selected for the design of second-generation CAR constructs. ScFvs were inserted into a CAR backbone containing an extracellular hinge and transmembrane region derived from the CD8α receptor fused to intracellular 4-1BB- (CD137-) co-stimulatory and CD3-ζ-activating signaling domains. Blue fluorescent protein (BFP) or a RQR8 polypeptide, which features two rituximab-binding domains and one Qbend10 recognition domain (anti-CD34 antibody),[31] was co-expressed with the CAR from lentiviral vectors via a ribosomal skip peptide to allow for detection using fluorescence or rituximab staining (Figure S1A). A tool BCMA CAR designed using a scFv from a publicly available sequence served as a positive control.

BCMA CAR T Candidates Exhibit Target-Dependent Cytokine Release and Comparable Distribution of T Cell Subsets

CAR Ts were produced from healthy donor T cells, and all cell products showed robust expression of the CAR as measured by flow cytometry (Figure 1A; Figure S2). High CAR expression and scFv-induced aggregation of CAR molecules have been reported to result in target-independent T cell activation (autoactivation or tonic signaling), accelerated T cell differentiation, and reduced long-term antitumor efficacy.[32–34] Release of interferon gamma (IFNγ) by CAR Ts was used as a surrogate for T cell activation. T cells cultured in the absence of target exhibited some spontaneous release of IFNγ (Figures S3A and S3B). However, a significant release of IFNγ was observed only in response to BCMA-expressing MM.1S cells (Figure S3B). Flow cytometry analysis of CD45RO and CD62L expression showed that all candidates had similar proportions of effector and memory cells within the CAR T population (Figures 1B and 1C).

BCMA CAR T Candidates Retain Effector Function upon Recursive Target Exposure and Demonstrate Potent Antitumor Activity *In Vivo*

The ability of CAR T candidates to kill cell lines expressing high and low levels of BCMA (Figure S4) was assessed in short-term (24 h) and long-term (7 day) cytotoxicity assay formats (Figures 1D–1F and Figures 1G–1I, respectively). In short-term assays, the candidate CAR Ts did not demonstrate cytotoxicity against BCMA-negative REH cells, but they exhibited robust dose-dependent cytotoxicity against the same cells transduced to express BCMA, as well as the multiple myeloma cell line MM.1S (Figures 1D–1F). All CAR T candidates performed comparably. Maintenance of CAR T-mediated cytotoxicity and proliferative ability in response to prolonged exposure to target cells has been reported to be associated with sustained antitumor activity.[35–37] In long-term assays, all CAR T candidates maintained appreciable cytotoxicity (Figures 1G–1I). BCMA 1 showed the highest degree of proliferation in response to co-culture with target cells for 7 days, while BCMA 2 showed the least (Figure 1J). It was noted that T cells from some donors exhibited strong proliferation and cytotoxicity regardless of the specific CAR construct expressed, whereas T cells from other donors failed to expand and had lower cytotoxicity when expressing BCMA 2 or BCMA 3 (Figure S5).

To attempt to further differentiate among BCMA CAR T candidates, *in vivo* orthotopic tumor models were developed in which animals received suboptimal doses of CAR Ts. Intravenous injection of luciferase-expressing MM.1S and Molp-8 tumor cell lines established highly aggressive disease in the bone marrow that was treated in a dose-responsive manner by CAR T infusion (Figures S6A and S6B). Unlike subcutaneous models, orthotopic implantation with these cell lines resulted in relapse, due to the development of secondary tumors in varied tissues, and, therefore, it represents an extremely stringent model (Figure S6C). Notably, these late recurrences were not always abrogated by increasing the initial T cell dose (Figure S6A). Because high numbers of T cell receptor (TCR)-expressing cells in some donors reduced tumor burden in a CAR-independent fashion (Figures S6A and S6C) and could potentially cause graft-versus-host (GvH) responses,[38–40] TALEN-mediated knockout of the TCR alpha constant (*TRAC*) locus was implemented to prevent xenogeneic responses[9] (Figures S6D and S6E). All three candidates showed high antitumor activity and an equivalent

flow cytometry using soluble BCMA (n = 5 donors). (K) BCMA CAR T candidates performed similarly in an orthotopic MM.1S tumor model. Tumor-bearing animals received 3×10^6 TCRα-deficient CAR$^+$ cells in a total of 1.8×10^7 cells. Tumor growth was assessed using whole-body luminescence imaging (n = 10 animals). (J) was analyzed using Tukey's one-way ANOVA and (K) was analyzed using Tukey's repeated-measures one-way ANOVA. All results are shown as mean ± SEM. Asterisks show statistical significance: *p < 0.05, **p < 0.01, ***p < 0.001, and ****p < 0.0001.

reduction of tumor burden (Figure 1K). This finding was consistent across a range of experiments employing two different donors (data not shown). In summary, all candidates were deemed to display appropriate characteristics, but given the higher consistency and slightly enhanced activity in some *in vitro* assays, BCMA 1 was chosen for further studies.

BCMA CAR Ts with an Intra-CAR Off Switch Maintain T Cell Memory Subsets and Antitumor Activity

A number of suicide genes enabling detection and selective elimination of CAR Ts using commercially available antibodies have been described.[31,41] Because expression of the RQR8 polypeptide may not be matched with that of the CAR,[13] rituximab recognition domains were incorporated directly into the CAR molecule, as recently described.[42] After different conformations were tested, a construct with two rituximab-binding domains located between the scFv and the hinge region of the CAR was chosen (BCMA 1-R2; Figure S1A). BCMA 1 (with RQR8) and BCMA 1-R2 CAR T were comparable in terms of transduction efficiency (Figure 2A) and retention of T cell memory phenotypes (Figures 2B and 2C). BCMA 1 and BCMA 1-R2 CAR Ts showed similar cytotoxicity against target cell lines in short-term assays (Figures 2D–2F). Furthermore, the CAR Ts performed equivalently in the long-term cytotoxicity test (Figures 2G–2I), and they showed similar target-dependent proliferation (Figure 2J). Tested side by side in an orthotopic model of multiple myeloma, no significant difference between BCMA 1 and BCMA 1-R2 was observed, although the kinetics of response appeared slightly different (Figure 2K).

Since BCMA can be shed from the surface of multiple myeloma cells, we evaluated the effect of soluble BCMA on BCMA 1-R2 CAR Ts, and we found no decrease in cytotoxicity with soluble BCMA (sBCMA) concentrations up to 100 ng/mL and only minimal decrease at 400 ng/mL (Figure S7A). We also investigated the possibility that rituximab binding to the BCMA 1-R2 CAR could induce clustering of the CAR, leading to T cell activation and activation-induced cell death (AICD). CAR Ts cultured for 24 h in the presence of rituximab displayed no changes in the expression of the activation marker 4-1BB, the T cell subset composition, or the frequency of Annexin V^+ cells, even at high concentrations (100 μg/mL) of the antibody (Figures S7B–S7D). Consistent with these observations, no increase in IFNγ was detected in cells cultured with rituximab for 24 h (<500 pg/mL; n = 3). From these data, it was concluded that incorporation of the off switch into the CAR did not dramatically alter CAR T phenotype or activity.

Intra-CAR Off Switch Mediates the Elimination of BCMA CAR Ts *In Vitro* and *In Vivo*

The functionality of the intra-CAR off switch depends on the ability of rituximab to faithfully recognize and bind to its mimotope. While detection with an anti-BCMA 1 scFv reagent (anti-idiotype antibody) showed a similar degree of staining between BCMA 1 and BCMA 1-R2, staining with rituximab was superior for BCMA 1-R2 (44.3% versus 27.6%; Figure 3A). In a complement-dependent cytotoxicity (CDC) assay, the improved detection of BCMA 1-R2 CAR Ts by rituximab correlated with improved depletion of these cells (Figure 3B). Cells that survived the assay were found to have low expression of the CAR (Figures 3C and 3D), indicating a direct correlation between expression levels of the off switch and CAR T depletion. Antitumor efficacy was completely abrogated by rituximab administration *in vivo*, and analysis of peripheral blood showed that rituximab treatment correlated with a loss of circulating CAR Ts (Figures 3E and 3F).

Disruption of the *TRAC* and *CD52* Genes Facilitates Allogeneic Therapy without Affecting T Cell Function

Lymphodepletion has been demonstrated in preclinical and clinical studies to enhance the efficacy of adoptive T cell therapy by temporarily eliminating suppressive immune cells, facilitating T cell expansion through higher availability of homeostatic cytokines, and eliminating anti-CAR T immune responses.[43–47] In the case of allogeneic cell therapies, lymphodepletion is even more critical since it may delay rejection of the allogeneic product. CD52 is widely expressed on immune cells, and the anti-CD52 antibody alemtuzumab is a clinically validated lymphodepletion agent.[48,49] Concurrent TALEN-mediated knockout of the *TRAC* and *CD52* genes has been shown to reduce the potential of graft-versus-host disease (GvHD)[9] and to render CD19-targeted CAR Ts resistant to alemtuzumab treatment, potentially providing a mechanism to use alemtuzumab to continue lymphodepleting the host and allowing CAR Ts to continue to function.

Using the same TALEN-knockout strategy, BCMA 1-R2 CAR Ts were generated with efficient knockout of *TRAC* and *CD52* (Figure 4A). After magnetic depletion of $TCR\alpha^+$ cells, less than 3% of $CD3^+$ cells were present in the final eluted fraction, providing a CAR T product of sufficient purity for research purposes, with the majority of the cells lacking expression of both CD3 and CD52 (Figures 4A and 4B). As a result, the purified cells were largely resistant to anti-CD52 antibody-induced CDC *in vitro* (Figure 4C). Gene-edited CAR Ts did not show altered T cell phenotypes compared to their wild-type counterparts (Figure 4D), and cytotoxic activity of BCMA 1-R2 CAR Ts *in vitro* was unaffected by gene knockout (Figure 4E). To test potential *in vivo* consequences of CD52 knockout, the activity of TCR/CD52-knockout CAR Ts was compared against TCR-knockout CAR Ts at a suboptimal T cell dose. Similar to the *in vitro* findings, dual gene editing did not lead to differences in antitumor activity (Figure 4F).

BCMA CAR Ts Show Durable Antitumor Activity in Mice Expressing Homeostatic Cytokines

As previously noted for other candidates, BCMA 1-R2 CAR Ts showed a dose-dependent antitumor effect *in vivo*, but disease recurrence was seen with most donors (Figure 5A). The kinetics of CAR Ts was examined in blood, and limited expansion and short-lived persistence were observed (Figure 5B). Retreatment of relapsed animals with CAR Ts demonstrated significant antitumor response (Figure 5C) and dramatic but short-lived expansion of CAR Ts

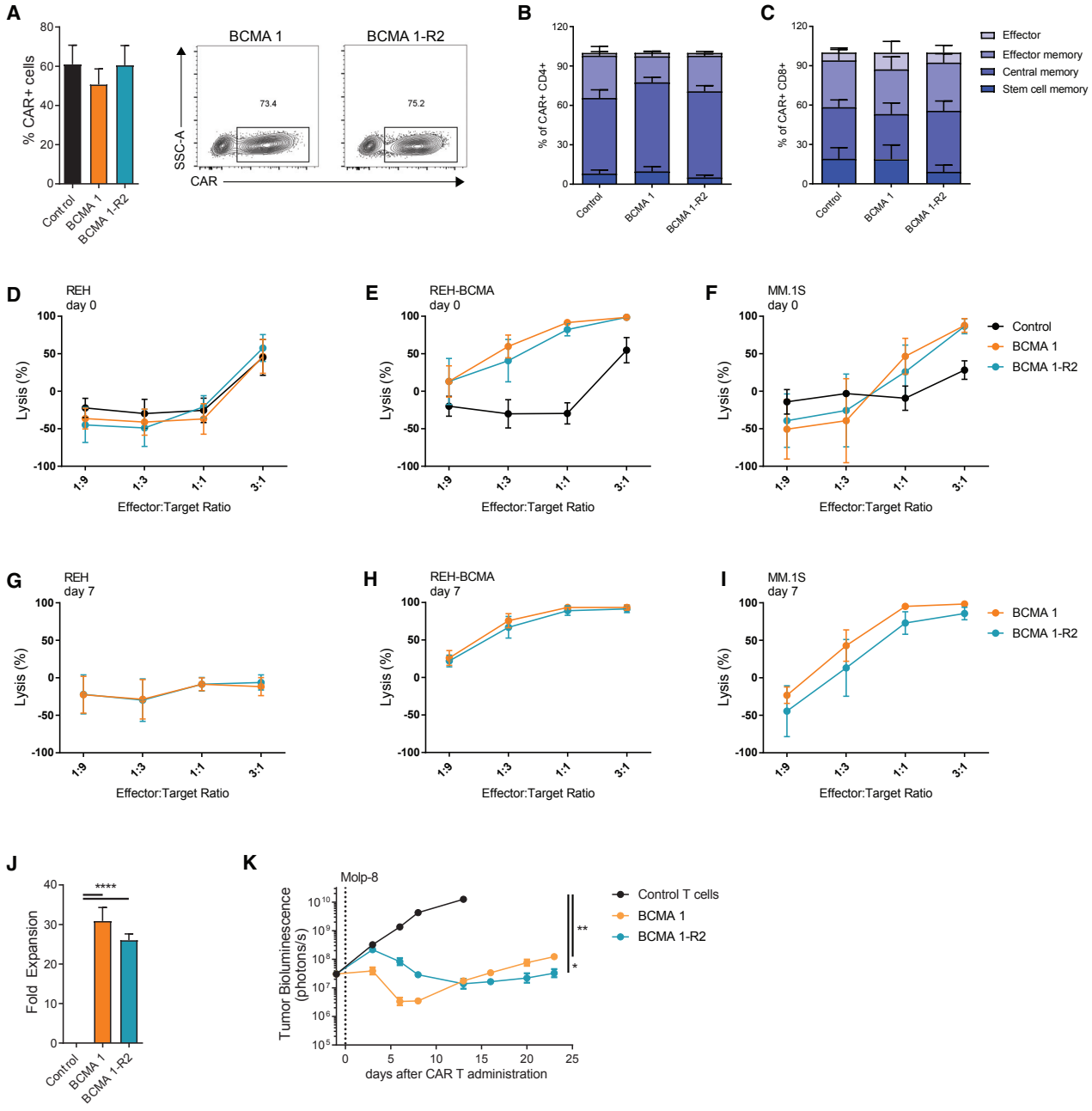

Figure 2. Incorporation of an Intra-CAR Off Switch Does Not Compromise the Efficacy of BCMA CAR Ts

(A) Addition of the off switch did not alter transduction efficiencies. BCMA CAR Ts were stained using soluble BCMA at day 14 of expansion and analyzed using flow cytometry (n = 5 donors). (B and C) Addition of the off switch did not alter CAR T differentiation. $CD4^+$ (B) and $CD8^+$ (C) CAR Ts were analyzed using flow cytometry 14 days after activation. Phenotypes were assigned according to CD62L and CD45RO expression within the CAR^+ population (n = 4 donors). (D–I) Addition of the off switch did not alter CAR T cytotoxicity. CAR Ts were cultured with luciferase-expressing BCMA-negative REH cells (D and G), REH cells overexpressing BCMA (E and H), or MM.1S cells (F and I). Target cell luminescence was assessed after 24 h. Cytotoxicity was determined immediately after recovery from cryopreservation (D–F) or after 3 rounds of expansion with BCMA-expressing target cells (G–I) (n = 5 donors). (J) Addition of the off switch did not affect CAR T proliferation. CAR Ts were expanded on BCMA-expressing target cells 3 times within 7 days and quantified by flow cytometry using soluble BCMA (n = 5 donors). (K) Addition of the off switch did not affect antitumor activity of BCMA CAR Ts in an orthotopic Molp-8 tumor model. Tumor-bearing animals received 3×10^6 TCRα-deficient CAR^+ cells (total of 3.8×10^6 cells), and tumor growth was assessed using whole-body luminescence imaging (n = 9–10 animals). (J) was analyzed using Tukey's one-way ANOVA and (K) was analyzed using Tukey's repeated-measures one-way ANOVA. All results are shown as mean ± SEM. Asterisks show statistical significance against the indicated condition: *$p < 0.05$, **$p < 0.01$, ***$p < 0.001$, and ****$p < 0.0001$.

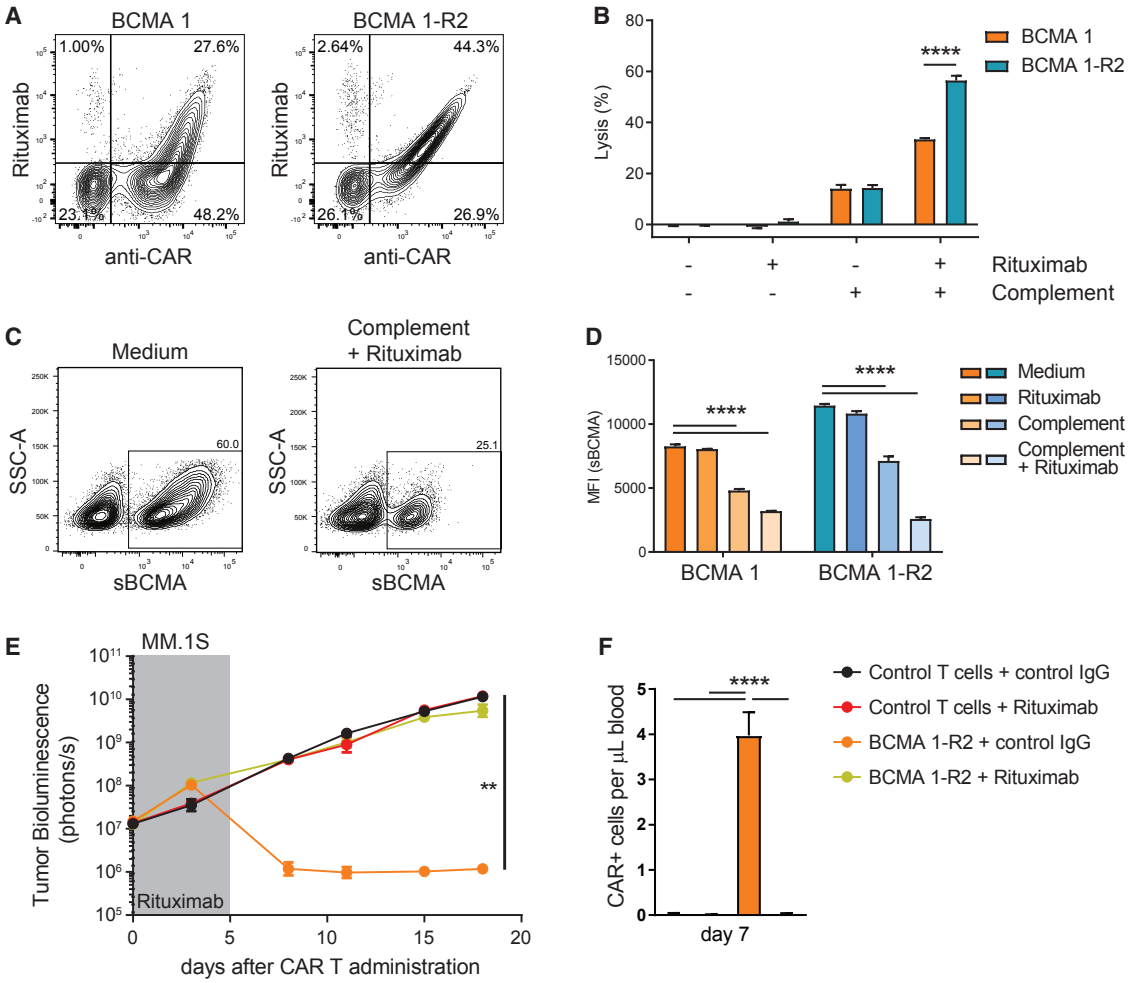

Figure 3. Intra-CAR Off Switch Allows Depletion of BCMA CAR Ts with Rituximab

(A) Intra-CAR CD20 mimotopes improve detection by rituximab. BCMA 1 CAR Ts (expressing RQR8) and BCMA 1-R2 CAR Ts were stained with anti-CAR antibody and rituximab 14 days after expansion and analyzed using flow cytometry. Numbers in quadrants represent percentages of total cells. (B) Intra-CAR off switch improved rituximab-mediated CDC. CAR Ts were incubated for 3 h with complement and rituximab, and cytotoxicity was assessed using flow cytometry (n = 3 donors). (C) Cells with higher CAR expression show higher susceptibility to rituximab in CDC assays. BCMA 1-R2 CAR Ts were cultured with and without the addition of complement and rituximab for 3 h and stained with soluble BCMA. Representative fluorescence-activated cell sorting (FACS) plots are shown. (D) Quantification of CAR mean fluorescence intensity, n = 3 technical replicates, representative experiment of 3 donors. (E) Rituximab treatment abrogated antitumor activity of TCRα-deficient BCMA 1-R2 CAR Ts in an orthotopic MM.1S tumor model. Tumor-bearing animals received 5×10^6 CAR$^+$ cells (total of 8.9×10^6 cells) followed by 5 consecutive daily injections of rituximab or control IgG (10 mg/kg). Tumor growth was assessed using whole-body luminescence imaging (n = 10 animals). (F) Rituximab treatment eliminated circulating BCMA CAR Ts in tumor-bearing mice. Peripheral blood of mice in (E) was collected 7 days after CAR T dosing and 2 days after the last rituximab injection, stained using soluble BCMA, and analyzed using flow cytometry (n = 6–9 mice). (B) was analyzed using paired t tests, (D) was analyzed using Dunnett's one-way ANOVA, (E) was analyzed using Tukey's repeated-measures one-way ANOVA, and (F) was analyzed using Tukey's one-way ANOVA. All results are shown as mean ± SEM. Asterisks show statistical significance against the indicated condition: *p < 0.05, **p < 0.01, ***p < 0.001, and ****p < 0.0001.

(Figure 5D). These results suggest that the failure in long-term efficacy of the initial CAR T infusion was not due to segregation of tumors at inaccessible locations or downregulation of BCMA expression by the tumor cells but likely the result of poor long-term engraftment and/or activity of human CAR Ts in this model.

The homeostatic cytokines IL-7 and IL-15 are required for human T cell survival and function,[43,50–54] and systemic concentration has been correlated to CAR T expansion in clinical trials.[55] To assess the role of these cytokines on CAR T expansion and survival, wild-type luciferase-labeled BCMA CAR Ts were tested in animals supplemented with recombinant human cytokines stabilized by antibodies or receptor-fragment crystallizable (Fc) fusion proteins.[56–59] IL-15 signaling was superior to IL-7 in increasing CAR T expansion (Figure S8A), which resulted in complete antitumor responses (Figure S8B).

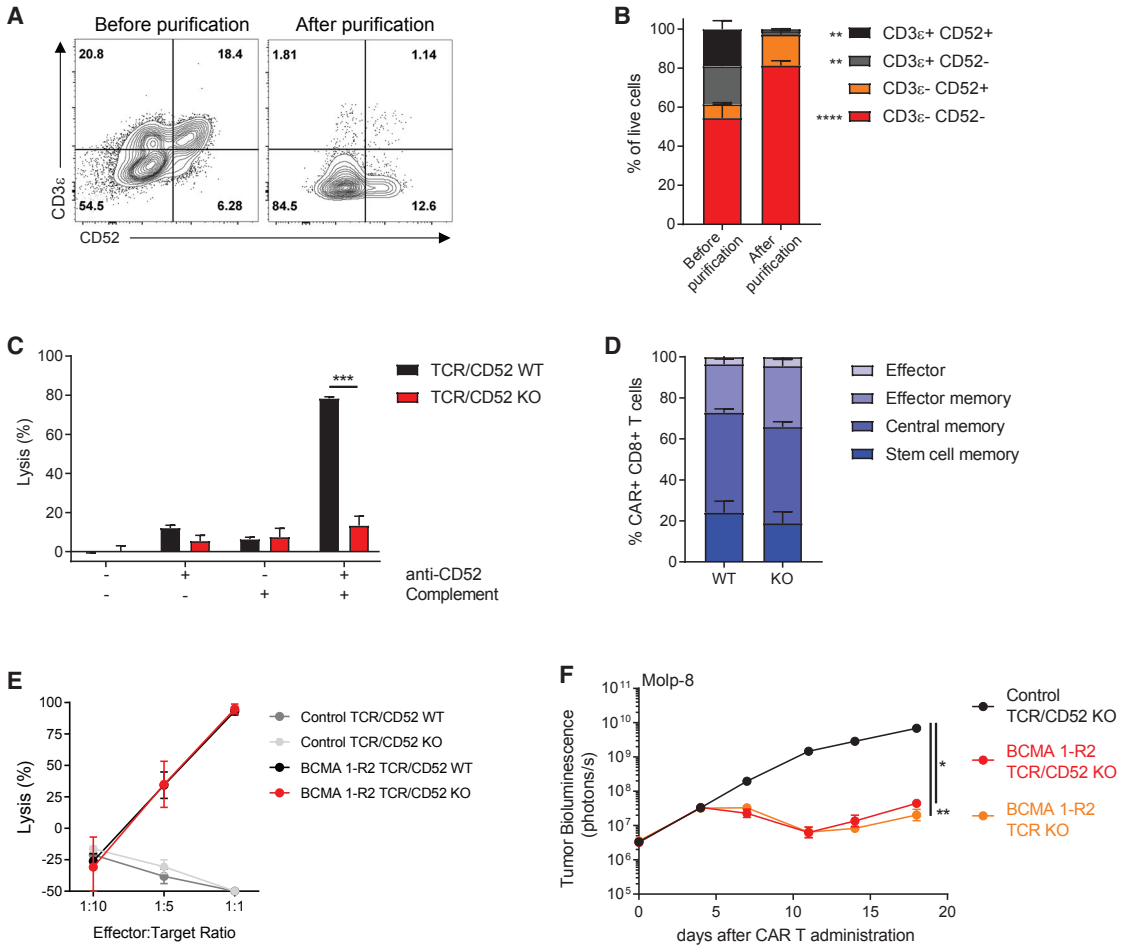

Figure 4. Gene Editing of BCMA CAR Ts Confers Resistance to Anti-CD52 Antibody Treatment without Affecting T Cell Function

(A and B) TALEN gene editing of the *TRAC* and *CD52* genes followed by magnetic depletion of residual TCRα$^+$ cells results in a CAR T product highly enriched for TCRα$^-$ and CD52$^-$ cells. At 14 days after expansion and either before or after purification with a TCRαβ selection kit, TALEN-treated BCMA 1-R2 CAR Ts were stained for the presence of CD3ε (as a surrogate for the TCRαβ complex) and for CD52, then analyzed using flow cytometry. (A) Relative composition of a representative donor CAR T product before and after purification and (B) comparison of the proportions of T cells expressing CD3ε and/or CD52 before and after purification across 3 donors. (C) Gene-edited BCMA CAR Ts are resistant to anti-CD52 antibodies. CAR Ts were incubated for 3 h with complement and anti-CD52 antibody, and cytotoxicity was assessed using flow cytometry (n = 3 donors). (D) Gene editing did not affect the differentiation of BCMA CAR Ts. CAR Ts were stained for CD45RO and CD62L 14 days after expansion and analyzed using flow cytometry (n = 3 donors). (E) Gene editing did not alter BCMA CAR T cytotoxicity *in vitro*. CAR Ts were cultured with luciferase-expressing REH cells overexpressing BCMA at the indicated ratios for 24 h (n = 3 donors). (F) Gene editing did not alter the activity of BCMA CAR Ts in an orthotopic Molp-8 tumor model. Tumor-bearing animals received 3 × 10^6 CAR$^+$ cells (total of 5.1 × 10^6 cells), and tumor growth was assessed using whole-body luminescence imaging (n = 9–10 animals). (B) was analyzed using Bonferroni two-way ANOVA, (C) was analyzed using t tests, and (F) was analyzed using Tukey's repeated-measures one-way ANOVA. All results are shown as mean ± SEM. Asterisks show statistical significance against the indicated condition: *p < 0.05, **p < 0.01, ***p < 0.001, and ****p < 0.0001.

To determine the influence of physiological cytokine concentrations on CAR T proliferation and antitumor activity *in vivo*, recombinant adeno-associated viruses designed to express human IL-7 and human IL-15/IL-15Rα complexes were injected into NSG mice. Adeno-associated virus (AAV)9-treated mice exhibited a steady and dose-dependent expression of these cytokines (Figures S8C and S8D). In the presence of physiological concentrations of IL-7 and IL-15, allogeneic BCMA 1-R2 CAR Ts exhibited durable antitumor activity (Figure 5E), accompanied by higher expansion and long-lived persistence of BCMA CAR Ts in peripheral blood (Figure 5F). To validate these findings, two additional BCMA CAR T candidates (BCMA 4-R2 and BCMA 5-R2) that had shown appropriate phenotype and high efficacy across a panel of *in vitro* and *in vivo* models (Figure S9) were tested. In the presence of cytokines, both candidates demonstrated enhanced antitumor activity, with BCMA 5-R2 CAR Ts showing deeper and longer-lived antitumor responses (Figure 5G). Based on the robust activity shown in this model, BCMA 1-R2 and BCMA 5-R2 were selected for further evaluation against a BCMA CAR that has been shown to mediate complete responses in clinical trials,[25] and they were found to have equivalent short-term and

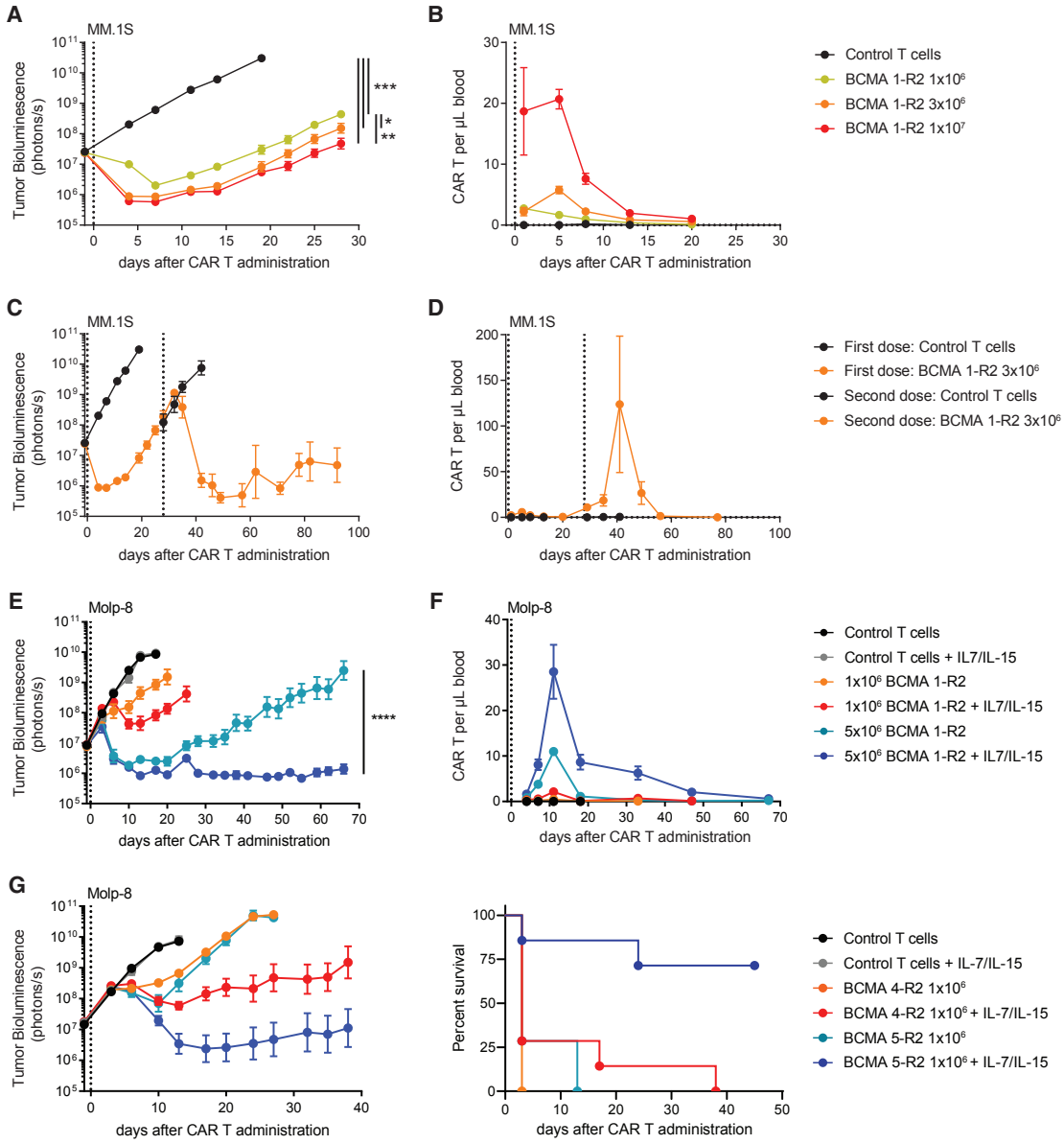

Figure 5. Homeostatic Cytokines Support BCMA CAR T Function by Enhancing Persistence in NSG Mice

(A and B) Orthotopic MM.1S tumor models were characterized by relapse of tumors and loss of BCMA CAR Ts in peripheral blood. (A) Tumor-bearing animals received the indicated doses of gene-edited CAR$^+$ cells (total of 11.5 × 10^6 cells), and tumor growth was assessed using whole-body luminescence imaging (n = 8–10 animals). (B) Peripheral blood BCMA CAR Ts were enumerated by flow cytometry (n = 2–5 animals/time point). (C and D) Successful treatment of relapsed tumors with a second dose of BCMA CAR Ts was accompanied by a strong expansion of CAR Ts in the peripheral blood. (C) Tumor-bearing mice from the 3 × 10^6-dose group in (A) received a second dose of 3 × 10^6 CAR$^+$ cells produced from the same donor (total of 5.1 × 10^6 cells), and tumor growth was assessed using whole-body luminescence imaging (n = 5 animals). (D) Peripheral blood BCMA CAR Ts of animals in (C) were enumerated by flow cytometry (n = 5 animals). (E) Homeostatic cytokines support BCMA CAR T activity and persistence in an orthotopic Molp-8 tumor model. NSG mice received AAV9 virus expressing human IL-7 (5 × 10^{10} genomic contents/animal) and human IL-15/IL-15Rα fusion proteins (5 × 10^{11} genomic contents/animal) 5 days prior to implantation of Molp-8 tumor cells. Tumor-bearing animals (mean cytokine concentrations of 16.7 ± 1.09 pg/mL IL-7 and 15.1 ± 0.86 pg/mL IL-15) received the indicated doses of BCMA CAR Ts produced with the clinical-scale protocol (total of 8.9 × 10^6 cells), and tumor growth was assessed using whole-body luminescence imaging (n = 8–10 animals). (F) Peripheral blood BCMA CAR Ts of the animals in (E) were enumerated by flow cytometry (n = 8–10 animals). (G) Homeostatic cytokines enable *in vivo* discrimination of otherwise equally effective BCMA CAR T candidates. NSG mice received AAV9 virus expressing human IL-7 (5 × 10^{11} genomic contents/animal) and human IL-15/IL-15Rα fusion proteins (5 × 10^{12} genomic contents/animal) 5 days prior to implantation of Molp-8 tumor cells. Tumor-bearing animals (mean cytokine concentrations of 200 ± 14.2 pg/mL IL-7 and 165 ± 7.2 pg/mL IL-15) received the indicated doses of BCMA CAR Ts (total of 2.3 × 10^6 cells). T cells in this experiment were not gene edited (n = 5–8 animals). (A), (C), (E), and (G) were analyzed using Tukey's repeated-measures one-way ANOVA. All results are shown as mean ± SEM. Asterisks show statistical significance against the indicated condition: *p < 0.05, **p < 0.01, ***p < 0.001, and ****p < 0.0001.

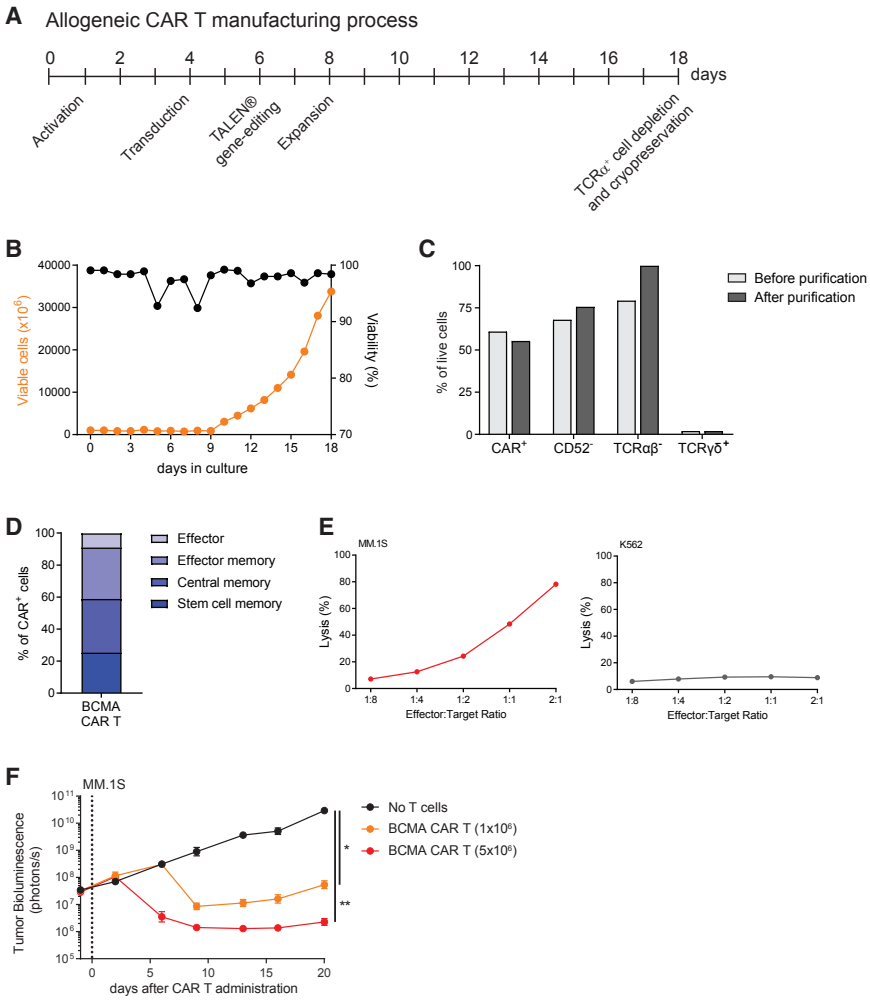

Figure 6. Large-Scale Manufacturing of Clinical-Grade Allogeneic BCMA CAR Ts with Potent Antitumor Activity

(A) Schematic representation of the manufacturing process. Allogeneic BCMA CAR Ts were generated using PBMCs derived from healthy donors following a GMP-grade process that results in a cryopreserved product with high antitumor efficacy and reduced potential for TCRαβ-mediated GvHD. (B) T cells transduced with the BCMA CAR displayed robust expansion in bioreactors and showed high viability over the entire process, except for transient and minimal changes associated with the transduction and gene-editing steps. (C) Bar graphs represent the percentage of T cells among live cells expressing the BCMA CAR or lacking expression of CD52 or TCRαβ, before and after depletion of residual TCRα$^+$ cells. The percentages of residual TCRγδ$^+$ T cells are also shown for comparison. (D) At the time of cryopreservation, the BCMA CAR T product contained a high frequency of cells expressing early memory markers, indicative of high proliferative potential. (E) BCMA CAR Ts exhibited cytotoxic activity against MM.1S cells, but they were not cytotoxic to BCMA-negative K562 cells. CAR Ts were cultured with luciferase-expressing target cells and luminescence was assessed after 24 h. (F) BCMA CAR Ts produced at large scale demonstrated potent antitumor activity in an orthotopic mouse model of multiple myeloma. Tumor-bearing animals received the indicated dose of CAR$^+$ cells (total of 10.9 × 10^6 cells), and tumor growth was assessed using whole-body luminescence imaging (n = 10 animals). Results were analyzed using Tukey's repeated-measures one-way ANOVA and are shown as mean ± SEM. Asterisks show statistical significance against the indicated condition: *p < 0.05 and **p < 0.01.

long-term killing activity (Figure S7E). Taken together, these results suggest that BCMA 1-R2 and BCMA 5-R2 are promising candidates for clinical evaluation.

Allogeneic BCMA CAR Ts Manufactured at Large Scale Preserve Their Phenotype and Antitumor Activity

Since large-scale manufacturing is a critical step in the development of off-the-shelf CAR T therapies, the phenotype and antitumor activity of BCMA CAR Ts produced in a proprietary good manufacturing practice (GMP)-like clinical-scale format (Figure 6A; Supplemental Materials and Methods) were evaluated. Activated T cells were effectively transduced with a concentrated lentivirus and displayed robust expansion in bioreactors (Figures 6B and 6C). Efficient inactivation of the *TRAC* and *CD52* genes using TALEN followed by magnetic depletion of residual TCRα$^+$ cells resulted in a final CAR T product highly enriched for TCRαβ$^-$ cells (Figure 6C), with over 50% of CAR Ts displaying a stem cell memory or central memory phenotype (Figure 6D). Furthermore, allogeneic BCMA CAR Ts manufactured at large scale exhibited dose-dependent cytotoxic activity *in vitro* (Figure 6E), and they mediated potent antitumor responses *in vivo* (Figure 6F). We conclude that allogeneic BCMA CAR Ts can be manufactured at large scale under GMP-like conditions with preservation of therapeutic potential.

DISCUSSION

In this report, a platform for allogeneic BCMA CAR Ts was developed. Candidate BCMA CARs were profiled in a variety of assays that evaluated manufacturability, activation in the absence of target cells, and long-term cytotoxic activity *in vitro* and *in vivo*. All five BCMA CARs tested were characterized by low tonic signaling, resulting in CAR Ts with high proliferative capacity and maintenance of cytotoxicity in long-term assays. Patient-derived CAR Ts have been shown to demonstrate reduced potency relative to healthy donor-derived cells.[6–8] CAR T proliferation and cytotoxicity were more pronounced for certain donors, which appeared to have a larger pool of memory cells at the beginning of the assays. The results shown here suggest that, even within subsets of healthy donors, differences in T cell potency exist. Since even CARs with a low level of autoactivation showed worse performance in some donors, care was taken to choose CARs that had consistent

activity across donors to minimize batch-to-batch variation in performance.

Co-expression of several genes by the same viral vector can dramatically reduce transduction efficiency and manufacturability of the product, and a suicide gene may not be co-expressed equivalently. An off switch incorporated into the CAR architecture could, therefore, overcome these potential obstacles. Here an intra-CAR rituximab-binding domain, which allows the depletion of CAR Ts using an FDA-approved reagent, was utilized.[42] The intra-CAR off switch did not alter CAR T function, and efficient rituximab-based elimination of CAR Ts was demonstrated. We found a direct correlation between CAR expression level and susceptibility to rituximab-induced CDC. It is possible that CAR Ts that are less efficiently bound by rituximab and, therefore, not depleted *in vitro* could be targeted via complementary effector mechanisms *in vivo*, such as antibody-dependent cellular cytotoxicity (ADCC), which has been shown to eliminate cells with a lower expression of CD20.[60]

Allogeneic CAR Ts could potentially overcome limitations of autologous CAR Ts by being available as an off-the-shelf product, but they have the potential to elicit GvHD when recognizing foreign major histocompatibility complex (MHC) molecules on the host tissues through the TCR complex. As demonstrated previously for CD19-directed CAR Ts,[9] we show here that TALEN-mediated knockout of the *TRAC* locus prevented xenogeneic GvHD responses in mice. Conversely, preventing rejection of the infused allogeneic CAR T product by host T and natural killer (NK) cells may require prolonged lymphodepletion. Simultaneous editing of the *CD52* locus rendered BCMA CAR Ts resistant to the FDA-approved lymphodepleting antibody alemtuzumab, allowing the possibility for extending the window of immunosuppression if required for full therapeutic efficacy.

Developing *in vitro* assays that predict *in vivo* function is of particular importance for the screening of large numbers of clinical CAR T candidates before conducting *in vivo* studies. Proliferation and long-term persistence of CAR Ts have been demonstrated to be the best correlators to therapeutic efficacy in preclinical studies,[36,37] and, in this study, *in vitro* assays that assessed proliferative capacity of the CAR T candidates in multiple donors were initially the best discriminator of CAR T activity, as *in vivo* experiments carried out in the absence of cytokine supplementation were not able to reveal differences. CAR T expansion was very limited in the orthotopic disease models, and loss of CAR Ts in the blood coincided with a recurrence of disease at metastatic sites. The homeostatic cytokines IL-7 and IL-15 maintain survival and function of human T cells,[43,50,51,53] and the lack of these cytokines in immunocompromised mice has been shown to impair the function of human T cells.[52] In line with previous studies employing human T cells,[54] physiological concentrations of IL-7 and IL-15 dramatically improved CAR T antitumor activity and persistence, allowing the distinction between two CAR T candidates with otherwise similar *in vitro* and *in vivo* activity.

Recent clinical trials employing autologous BCMA CAR Ts demonstrate the feasibility and therapeutic potential of CAR T therapies in patients with relapsed or refractory multiple myeloma.[61] Allogeneic BCMA CAR Ts produced at a large scale showed potent antitumor activity and durability of response, supporting a clinical investigation in this patient population with a high unmet need.

MATERIALS AND METHODS

Construction of Lentiviral Vectors Encoding anti-BCMA CARs

Antibodies toward BCMA were obtained by panning a synthetic human phage-display library, and their affinities were determined by surface plasmon resonance (SPR). Higher-affinity antibodies were generated by affinity maturation, and five antibodies that bound to overlapping epitopes on BCMA with nanomolar affinities were considered for further evaluation and design of the CAR constructs (Table S1; Supplemental Materials and Methods). Lentiviral transfer vectors encoding RQR8-2A-CAR (candidate scFv), BFP-2A-CAR (tool CAR; GenBank: AOC20704.1 and AOC20765.1), and BFP-2A-STOP (control) were sourced from Cellectis SA. The nucleotide sequences encoding the BCMA-R2 CARs were synthesized and replaced the IRES-Puro cassette in the pLVX-EF1α-IRES-puro vector (Takara Bio, Mountain View, CA). All transfer vectors encoded the CAR under regulatory control of the EF1α promoter and the woodchuck hepatitis virus post-transcriptional regulatory element (WPRE).

CAR T Production

Detailed description of the production methodology can be found in the Supplemental Materials and Methods. Briefly, T cells were activated immediately after recovery from cryopreservation in X-Vivo15 medium (Lonza, Basel, Switzerland), supplemented with 10% fetal calf serum (FCS) (GE Healthcare, Pittsburgh, PA) and 20 ng/mL IL-2 (Miltenyi Biotec, Auburn, CA), using T cell TransAct (Miltenyi Biotec, Auburn, CA) as recommended by the manufacturer. T cells were transduced with neat lentiviral supernatant 2 days after activation and then cultured in X-Vivo15 medium supplemented with 5% human AB serum (Gemini Bio-Products, West Sacramento, CA). IL-2 was supplemented every 2–3 days. At 7 days after activation, T cells were transfected with 25 μg/mL/TRAC and CD52 TALEN monomer mRNA (TriLink Biotechnologies, San Diego, CA), using AgilePulse MAX electroporators (BTX, Holliston, MA). At 17 days after activation, depletion of TCRα-positive cells was performed using TCRα/β cell isolation kits (Miltenyi Biotec, Auburn, CA). At 18 days after activation, T cells were cryopreserved in 90% FCS/10% DMSO using rate-controlled freezing chambers and stored in liquid nitrogen vapor phase.

For large-scale production, healthy donor-derived peripheral blood mononuclear cells (PBMCs) (Hemacare, Los Angeles, CA) were activated 24 h after thawing. Cells were transduced 3 days after activation with a concentrated lentiviral vector (Miltenyi Biotec, Auburn, CA), encoding one of the CARs shown in Table S1, and electroporated with TALEN mRNA 5 days after activation. At 7 days after activation, cells were expanded in 2L WAVE bag bioreactors (GE Healthcare,

Pittsburgh, PA). Depletion of TCRα^+ cells was performed using CliniMACS Prodigy (Miltenyi Biotec, Auburn, CA), and T cells were cryopreserved in CS5 cryoprotectant (STEMCELL Technologies, Vancouver, BC, Canada). All functional assays were performed with cells after recovery from cryopreservation.

Flow Cytometry Analysis

Blood samples were treated twice with red blood cell lysis buffer (BioLegend, San Diego, CA). Cells were stained using conventional flow cytometry protocols in Brilliant Stain buffer (BD Biosciences, San Jose, CA), supplemented with human TruStain Fc blocking reagent (BioLegend, San Diego, CA). The following reagents were used: anti-human CD45RO allophycocyanin (APC), anti-human CD62L BV605, anti-human CD8a BV510, anti-human CD4 BV785, anti-human TCRαβ antibody phycoerythrin (PE), anti-human CD3 antibody BUV395 or fluorescein isothiocyanate (FITC), anti-human CD269 PE, anti-Mouse CD45 APC/Cy7 (BioLegend, San Diego, CA), Streptavidin PE (BioLegend, San Diego, CA), soluble biotinylated BCMA, rituximab PE, anti-human CD52 PE, and anti-BCMA 1 idiotype PE (produced in-house). Dead cells were stained using Zombie NIR (BioLegend, San Diego, CA), and cells were fixed with intracellular (IC) fixation buffer (Thermo Fisher Scientific, Waltham, MA). Samples were supplemented with counting beads (Thermo Fisher Scientific, Waltham, MA) prior to analysis using Fortessa LSRII flow cytometers (BD Biosciences, San Jose, CA).

Short-Term Cytotoxicity and Cytokine Production Assays

2×10^4 luciferase-expressing target cells were co-cultured with effector cells in RPMI 1640 medium supplemented with 10% FCS at defined effector-to-target ratios for 24 h. Culture supernatants were analyzed for the presence of IFNγ using Human IFN-Gamma Quantikine Kit (R&D Systems, Minneapolis, MN). Target cell survival was assessed using ONE-Glo reagent (Promega, Madison, WI).

Long-Term Cytotoxicity and Proliferation Assay

2×10^6 luciferase-expressing MM.1S cells and 5×10^5 CAR$^+$ T cells were co-cultured in RPMI 1640 medium supplemented with 10% FCS in 24-well G-rex plates (Wilson Wolf, St. Paul, MN). Every 48 h, CAR Ts were counted and re-suspended in fresh medium with an equal number of new target cells. After three rounds of target exposure, CAR Ts were stained using soluble BCMA and quantified by flow cytometry. CAR Ts were then tested using the short-term cytotoxicity assay.

Complement-Dependent Cytotoxicity Assay

2×10^5 cells were incubated in RPMI 1640 medium supplemented with 10% FCS in 48-well plates. Cells were incubated for 3 h in the absence or presence of 25% baby rabbit complement (Bio-Rad, Hercules, CA) and anti-CD52 or rituximab antibodies (produced in-house; 100 μg/mL). Cells were stained with soluble BCMA or CD3 antibodies, and cytotoxicity was analyzed by flow cytometry.

In Vivo Studies

All procedures performed on animals were in accordance with regulations and established guidelines and were reviewed and approved by an Institutional Animal Care and Use Committee. 8- to 12-week-old NSG mice were obtained from Jackson Laboratory (Bar Harbor, ME). Animals were irradiated with 1 Gy 1 day prior to intravenous injection of either 2×10^6 Molp-8 cells or 5×10^6 MM.1S cells. In some cases, animals received injections of titrated AAV9 viruses (Vigene Biosciences, Rockville, MD) coding for human IL-7 or human IL-15/IL-15Rα fusion proteins under the control of an EF1α promoter 4 days prior to irradiation. Tumor burden was measured using an IVIS Spectrum instrument (PerkinElmer, Boston, MA) twice weekly. Animals were randomized based on total body bioluminescence 8–12 days (Molp-8) or 14 days (MM.1S) after tumor cell injection, unless stated otherwise, and CAR Ts were injected immediately after thawing. Total T cell numbers were kept constant across all groups by adding untransduced T cells, unless stated otherwise. Where indicated, animals received intraperitoneal injections of 10 mg/kg rituximab or isotype control antibody (immunoglobulin G [IgG]1). Blood was collected into EDTA-coated tubes using submandibular bleeds, and 50 μL was used for flow cytometry. Animals were euthanized if they exhibited disease model-specific endpoints such as hind-leg paralysis, ruffled fur, or 20% of body weight loss. Relapse was defined as the first time point after nadir that an individual mouse's tumor bioluminescence was higher than the total flux measured at the time of CAR T dosing. Time to progression was defined as the time between CAR T dosing and relapse, and it was used to estimate progression-free survival curves.

Statistical Analysis

Statistical analysis was performed using the Prism software package (GraphPad, San Diego, CA), and statistical tests used are indicated in the figure legends. All tests were two-sided and $p < 0.05$ was considered significant.

SUPPLEMENTAL INFORMATION

Supplemental Information can be found online at https://doi.org/10.1016/j.ymthe.2019.04.001.

AUTHOR CONTRIBUTIONS

C.S., B.B., T.C.K., T.B., J. Sutton, A.C., T.G., H.D., R.G., and A.G. performed CAR T experiments. E.P., C.B., S.M.C., T.S., and T.V.B. created antibodies and protein reagents. C.S., B.B., T.C.K., R.G., A.J., J.V., P.D., J. Smith, T.P., Y.N., A.R., T.V.B., J.C.-R., and B.J.S. designed the studies and interpreted the data. C.S., B.B., and B.J.S. wrote the manuscript and are responsible for the integrity of the work as a whole.

CONFLICTS OF INTEREST

All authors are current or former employees of Allogene Therapeutics, Inc.; Pfizer Inc.; Cellectis SA; or Cellectis, Inc.

ACKNOWLEDGMENTS

We thank Mark Leonard and his team for providing the BCMA CAR Ts produced at large scale for *in vivo* testing. We thank German Vergara and Teresa Radcliffe and their teams for support with the animal

studies and Kevin Lindquist and Marjorie Bateman for support with the SPR assays.

REFERENCES

1. Neelapu, S.S., Locke, F.L., Bartlett, N.L., Lekakis, L.J., Miklos, D.B., Jacobson, C.A., Braunschweig, I., Oluwole, O.O., Siddiqi, T., Lin, Y., et al. (2017). Axicabtagene ciloleucel CAR T-cell therapy in refractory large B-cell lymphoma. N. Engl. J. Med. *377*, 2531–2544.
2. Maude, S.L., Laetsch, T.W., Buechner, J., Rives, S., Boyer, M., Bittencourt, H., Bader, P., Verneris, M.R., Stefanski, H.E., Myers, G.D., et al. (2018). Tisagenlecleucel in children and young adults with B-cell lymphoblastic leukemia. N. Engl. J. Med. *378*, 439–448.
3. Moro-García, M.A., Alonso-Arias, R., and López-Larrea, C. (2013). When aging reaches CD4+ T-cells: phenotypic and functional changes. Front. Immunol. *4*, 107.
4. Palmer, S., Albergante, L., Blackburn, C.C., and Newman, T.J. (2018). Thymic involution and rising disease incidence with age. Proc. Natl. Acad. Sci. USA *115*, 1883–1888.
5. Salam, N., Rane, S., Das, R., Faulkner, M., Gund, R., Kandpal, U., Lewis, V., Mattoo, H., Prabhu, S., Ranganathan, V., et al. (2013). T cell ageing: effects of age on development, survival & function. Indian J. Med. Res. *138*, 595–608.
6. Singh, N., Perazzelli, J., Grupp, S.A., and Barrett, D.M. (2016). Early memory phenotypes drive T cell proliferation in patients with pediatric malignancies. Sci. Transl. Med. *8*, 320ra3.
7. Fraietta, J.A., Beckwith, K.A., Patel, P.R., Ruella, M., Zheng, Z., Barrett, D.M., Lacey, S.F., Melenhorst, J.J., McGettigan, S.E., Cook, D.R., et al. (2016). Ibrutinib enhances chimeric antigen receptor T-cell engraftment and efficacy in leukemia. Blood *127*, 1117–1127.
8. Hoffmann, J.M., Schubert, M.L., Wang, L., Hückelhoven, A., Sellner, L., Stock, S., Schmitt, A., Kleist, C., Gern, U., Loskog, A., et al. (2018). Differences in expansion potential of naive chimeric antigen receptor T cells from healthy donors and untreated chronic lymphocytic leukemia patients. Front. Immunol. *8*, 1956.
9. Poirot, L., Philip, B., Schiffer-Mannioui, C., Le Clerre, D., Chion-Sotinel, I., Derniame, S., Potrel, P., Bas, C., Lemaire, L., Galetto, R., et al. (2015). Multiplex genome-edited T-cell manufacturing platform for "off-the-shelf" adoptive T-cell immmunotherapies. Cancer Res. *75*, 3853–3864.
10. Cooper, M.L., Choi, J., Staser, K., Ritchey, J.K., Devenport, J.M., Eckardt, K., Rettig, M.P., Wang, B., Eissenberg, L.G., Ghobadi, A., et al. (2018). An "off-the-shelf" fratricide-resistant CAR-T for the treatment of T cell hematologic malignancies. Leukemia *32*, 1970–1983.
11. Gautron, A.S., Juillerat, A., Guyot, V., Filhol, J.M., Dessez, E., Duclert, A., Duchateau, P., and Poirot, L. (2017). Fine and predictable tuning of TALEN gene editing targeting for improved T cell adoptive immunotherapy. Mol. Ther. Nucleic Acids *9*, 312–321.
12. Georgiadis, C., Preece, R., Nickolay, L., Etuk, A., Petrova, A., Ladon, D., Danyi, A., Humphryes-Kirilov, N., Ajetunmobi, A., Kim, D., et al. (2018). Long terminal repeat CRISPR-CAR-coupled "universal" T cells mediate potent anti-leukemic effects. Mol. Ther. *26*, 1215–1227.
13. Qasim, W., Zhan, H., Samarasinghe, S., Adams, S., Amrolia, P., Stafford, S., Butler, K., Rivat, C., Wright, G., Somana, K., et al. (2017). Molecular remission of infant B-ALL after infusion of universal TALEN gene-edited CAR T cells. Sci. Transl. Med. *9*, eaaj2013.
14. Graham, C., Yallop, D., Jozwik, A., Patten, P., Dunlop, A., Ellard, R., Stewart, O., Potter, V., Metaxa, V., Kassam, S., et al. (2017). Preliminary results of UCART19, an allogeneic anti-CD19 CAR T-cell product, in a first-in-human trial (CALM) in adult patients with CD19+ relapsed/refractory B-cell acute lymphoblastic leukemia. Blood *130*, 887.
15. Palumbo, A., and Anderson, K. (2011). Multiple myeloma. N. Engl. J. Med. *364*, 1046–1060.
16. Sonneveld, P., and Broijl, A. (2016). Treatment of relapsed and refractory multiple myeloma. Haematologica *101*, 396–406.
17. Gross, J.A., Johnston, J., Mudri, S., Enselman, R., Dillon, S.R., Madden, K., Xu, W., Parrish-Novak, J., Foster, D., Lofton-Day, C., et al. (2000). TACI and BCMA are receptors for a TNF homologue implicated in B-cell autoimmune disease. Nature *404*, 995–999.
18. O'Connor, B.P., Raman, V.S., Erickson, L.D., Cook, W.J., Weaver, L.K., Ahonen, C., Lin, L.L., Mantchev, G.T., Bram, R.J., and Noelle, R.J. (2004). BCMA is essential for the survival of long-lived bone marrow plasma cells. J. Exp. Med. *199*, 91–98.
19. Tai, Y.T., Acharya, C., An, G., Moschetta, M., Zhong, M.Y., Feng, X., Cea, M., Cagnetta, A., Wen, K., van Eenennaam, H., et al. (2016). APRIL and BCMA promote human multiple myeloma growth and immunosuppression in the bone marrow microenvironment. Blood *127*, 3225–3236.
20. Seckinger, A., Delgado, J.A., Moser, S., Moreno, L., Neuber, B., Grab, A., Lipp, S., Merino, J., Prosper, F., Emde, M., et al. (2017). Target expression, generation, preclinical activity, and pharmacokinetics of the BCMA-T cell bispecific antibody EM801 for multiple myeloma treatment. Cancer Cell *31*, 396–410.
21. Ryan, M.C., Hering, M., Peckham, D., McDonagh, C.F., Brown, L., Kim, K.M., Meyer, D.L., Zabinski, R.F., Grewal, I.S., and Carter, P.J. (2007). Antibody targeting of B-cell maturation antigen on malignant plasma cells. Mol. Cancer Ther. *6*, 3009–3018.
22. Oden, F., Marino, S.F., Brand, J., Scheu, S., Kriegel, C., Olal, D., Takvorian, A., Westermann, J., Yilmaz, B., Hinz, M., et al. (2015). Potent anti-tumor response by targeting B cell maturation antigen (BCMA) in a mouse model of multiple myeloma. Mol. Oncol. *9*, 1348–1358.
23. Hipp, S., Tai, Y.T., Blanset, D., Deegen, P., Wahl, J., Thomas, O., Rattel, B., Adam, P.J., Anderson, K.C., and Friedrich, M. (2017). A novel BCMA/CD3 bispecific T-cell engager for the treatment of multiple myeloma induces selective lysis in vitro and in vivo. Leukemia *31*, 1743–1751.
24. Carpenter, R.O., Evbuomwan, M.O., Pittaluga, S., Rose, J.J., Raffeld, M., Yang, S., Gress, R.E., Hakim, F.T., and Kochenderfer, J.N. (2013). B-cell maturation antigen is a promising target for adoptive T-cell therapy of multiple myeloma. Clin. Cancer Res. *19*, 2048–2060.
25. Ali, S.A., Shi, V., Maric, I., Wang, M., Stroncek, D.F., Rose, J.J., Brudno, J.N., Stetler-Stevenson, M., Feldman, S.A., Hansen, B.G., et al. (2016). T cells expressing an anti-B-cell maturation antigen chimeric antigen receptor cause remissions of multiple myeloma. Blood *128*, 1688–1700.
26. Lee, L., Draper, B., Chaplin, N., Philip, B., Chin, M., Galas-Filipowicz, D., Onuoha, S., Thomas, S., Baldan, V., Bughda, R., et al. (2018). An APRIL-based chimeric antigen receptor for dual targeting of BCMA and TACI in multiple myeloma. Blood *131*, 746–758.
27. Bluhm, J., Kieback, E., Marino, S.F., Oden, F., Westermann, J., Chmielewski, M., Abken, H., Uckert, W., Höpken, U.E., and Rehm, A. (2018). CAR T cells with enhanced sensitivity to B cell maturation antigen for the targeting of B cell non-Hodgkin's lymphoma and multiple myeloma. Mol. Ther. *26*, 1906–1920.
28. Bu, D.X., Singh, R., Choi, E.E., Ruella, M., Nunez-Cruz, S., Mansfield, K.G., Bennett, P., Barton, N., Wu, Q., Zhang, J., et al. (2018). Pre-clinical validation of B cell maturation antigen (BCMA) as a target for T cell immunotherapy of multiple myeloma. Oncotarget *9*, 25764–25780.
29. Friedman, K.M., Garrett, T.E., Evans, J.W., Horton, H.M., Latimer, H.J., Seidel, S.L., Horvath, C.J., and Morgan, R.A. (2018). Effective targeting of multiple B-cell maturation antigen-expressing hematological malignances by anti-B-cell maturation antigen chimeric antigen receptor T cells. Hum. Gene Ther. *29*, 585–601.
30. Smith, E.L., Staehr, M., Masakayan, R., Tatake, J.J., Purdon, T.J., Wang, X., Wang, P., Liu, H., Xu, Y., Garrett-Thomson, S.C., et al. (2018). Development and evaluation of an optimal human single-chain variable fragment-derived BCMA-targeted CAR T cell vector. Mol. Ther. *26*, 1447–1456.
31. Philip, B., Kokalaki, E., Mekkaoui, L., Thomas, S., Straathof, K., Flutter, B., Marin, V., Marafioti, T., Chakraverty, R., Linch, D., et al. (2014). A highly compact epitope-based marker/suicide gene for easier and safer T-cell therapy. Blood *124*, 1277–1287.
32. Long, A.H., Haso, W.M., Shern, J.F., Wanhainen, K.M., Murgai, M., Ingaramo, M., Smith, J.P., Walker, A.J., Kohler, M.E., Venkateshwara, V.R., et al. (2015). 4-1BB costimulation ameliorates T cell exhaustion induced by tonic signaling of chimeric antigen receptors. Nat. Med. *21*, 581–590.
33. Frigault, M.J., Lee, J., Basil, M.C., Carpenito, C., Motohashi, S., Scholler, J., Kawalekar, O.U., Guedan, S., McGettigan, S.E., Posey, A.D., Jr., et al. (2015). Identification of chimeric antigen receptors that mediate constitutive or inducible proliferation of T cells. Cancer Immunol. Res. *3*, 356–367.

34. Gomes-Silva, D., Mukherjee, M., Srinivasan, M., Krenciute, G., Dakhova, O., Zheng, Y., Cabral, J.M.S., Rooney, C.M., Orange, J.S., Brenner, M.K., and Mamonkin, M. (2017). Tonic 4-1BB costimulation in chimeric antigen receptors impedes T cell survival and is vector-dependent. Cell Rep. *21*, 17–26.

35. Kalos, M., Levine, B.L., Porter, D.L., Katz, S., Grupp, S.A., Bagg, A., and June, C.H. (2011). T cells with chimeric antigen receptors have potent antitumor effects and can establish memory in patients with advanced leukemia. Sci. Transl. Med. *3*, 95ra73.

36. Kawalekar, O.U., O'Connor, R.S., Fraietta, J.A., Guo, L., McGettigan, S.E., Posey, A.D., Jr., Patel, P.R., Guedan, S., Scholler, J., Keith, B., et al. (2016). Distinct signaling of coreceptors regulates specific metabolism pathways and impacts memory development in CAR T cells. Immunity *44*, 380–390.

37. Zhao, Z., Condomines, M., van der Stegen, S.J.C., Perna, F., Kloss, C.C., Gunset, G., Plotkin, J., and Sadelain, M. (2015). Structural design of engineered costimulation determines tumor rejection kinetics and persistence of CAR T cells. Cancer Cell *28*, 415–428.

38. Alcantar-Orozco, E.M., Gornall, H., Baldan, V., Hawkins, R.E., and Gilham, D.E. (2013). Potential limitations of the NSG humanized mouse as a model system to optimize engineered human T cell therapy for cancer. Hum. Gene Ther. Methods *24*, 310–320.

39. Markley, J.C., and Sadelain, M. (2010). IL-7 and IL-21 are superior to IL-2 and IL-15 in promoting human T cell-mediated rejection of systemic lymphoma in immunodeficient mice. Blood *115*, 3508–3519.

40. Hu, B., Ren, J., Luo, Y., Keith, B., Young, R.M., Scholler, J., Zhao, Y., and June, C.H. (2017). Augmentation of antitumor immunity by human and mouse CAR T cells secreting IL-18. Cell Rep. *20*, 3025–3033.

41. Wang, X., Chang, W.C., Wong, C.W., Colcher, D., Sherman, M., Ostberg, J.R., Forman, S.J., Riddell, S.R., and Jensen, M.C. (2011). A transgene-encoded cell surface polypeptide for selection, in vivo tracking, and ablation of engineered cells. Blood *118*, 1255–1263.

42. Valton, J., Guyot, V., Boldajipour, B., Sommer, C., Pertel, T., Juillerat, A., Duclert, A., Sasu, B.J., Duchateau, P., and Poirot, L. (2018). A versatile safeguard for chimeric antigen receptor T-cell immunotherapies. Sci. Rep. *8*, 8972.

43. Gattinoni, L., Finkelstein, S.E., Klebanoff, C.A., Antony, P.A., Palmer, D.C., Spiess, P.J., Hwang, L.N., Yu, Z., Wrzesinski, C., Heimann, D.M., et al. (2005). Removal of homeostatic cytokine sinks by lymphodepletion enhances the efficacy of adoptively transferred tumor-specific CD8+ T cells. J. Exp. Med. *202*, 907–912.

44. Klebanoff, C.A., Khong, H.T., Antony, P.A., Palmer, D.C., and Restifo, N.P. (2005). Sinks, suppressors and antigen presenters: how lymphodepletion enhances T cell-mediated tumor immunotherapy. Trends Immunol. *26*, 111–117.

45. Wallen, H., Thompson, J.A., Reilly, J.Z., Rodmyre, R.M., Cao, J., and Yee, C. (2009). Fludarabine modulates immune response and extends in vivo survival of adoptively transferred CD8 T cells in patients with metastatic melanoma. PLoS ONE *4*, e4749.

46. Lamers, C.H., Willemsen, R., van Elzakker, P., van Steenbergen-Langeveld, S., Broertjes, M., Oosterwijk-Wakka, J., Oosterwijk, E., Sleijfer, S., Debets, R., and Gratama, J.W. (2011). Immune responses to transgene and retroviral vector in patients treated with ex vivo-engineered T cells. Blood *117*, 72–82.

47. Turtle, C.J., Hanafi, L.A., Berger, C., Hudecek, M., Pender, B., Robinson, E., Hawkins, R., Chaney, C., Cherian, S., Chen, X., et al. (2016). Immunotherapy of non-Hodgkin's lymphoma with a defined ratio of CD8+ and CD4+ CD19-specific chimeric antigen receptor-modified T cells. Sci. Transl. Med. *8*, 355ra116.

48. Demko, S., Summers, J., Keegan, P., and Pazdur, R. (2008). FDA drug approval summary: alemtuzumab as single-agent treatment for B-cell chronic lymphocytic leukemia. Oncologist *13*, 167–174.

49. Gärtner, F., Hieke, S., Finke, J., and Bertz, H. (2013). Lowering the alemtuzumab dose in reduced intensity conditioning allogeneic hematopoietic cell transplantation is associated with a favorable early intense natural killer cell recovery. Cytotherapy *15*, 1237–1244.

50. Rochman, Y., Spolski, R., and Leonard, W.J. (2009). New insights into the regulation of T cells by gamma(c) family cytokines. Nat. Rev. Immunol. *9*, 480–490.

51. Melchionda, F., Fry, T.J., Milliron, M.J., McKirdy, M.A., Tagaya, Y., and Mackall, C.L. (2005). Adjuvant IL-7 or IL-15 overcomes immunodominance and improves survival of the CD8+ memory cell pool. J. Clin. Invest. *115*, 1177–1187.

52. Drake, A., Kaur, M., Iliopoulou, B.P., Phennicie, R., Hanson, A., and Chen, J. (2016). Interleukins 7 and 15 maintain human T cell proliferative capacity through STAT5 signaling. PLoS ONE *11*, e0166280.

53. Nayar, S., Dasgupta, P., and Galustian, C. (2015). Extending the lifespan and efficacies of immune cells used in adoptive transfer for cancer immunotherapies-A review. OncoImmunology *4*, e1002720.

54. Huang, J., Li, X., Coelho-dos-Reis, J.G., Wilson, J.M., and Tsuji, M. (2014). An AAV vector-mediated gene delivery approach facilitates reconstitution of functional human CD8+ T cells in mice. PLoS ONE *9*, e88205.

55. Kochenderfer, J.N., Somerville, R.P.T., Lu, T., Shi, V., Bot, A., Rossi, J., Xue, A., Goff, S.L., Yang, J.C., Sherry, R.M., et al. (2017). Lymphoma remissions caused by anti-CD19 chimeric antigen receptor T cells are associated with high serum interleukin-15 levels. J. Clin. Oncol. *35*, 1803–1813.

56. Boyman, O., Ramsey, C., Kim, D.M., Sprent, J., and Surh, C.D. (2008). IL-7/anti-IL-7 mAb complexes restore T cell development and induce homeostatic T Cell expansion without lymphopenia. J. Immunol. *180*, 7265–7275.

57. Mortier, E., Quéméner, A., Vusio, P., Lorenzen, I., Boublik, Y., Grötzinger, J., Plet, A., and Jacques, Y. (2006). Soluble interleukin-15 receptor alpha (IL-15R alpha)-sushi as a selective and potent agonist of IL-15 action through IL-15R beta/gamma. Hyperagonist IL-15 x IL-15R alpha fusion proteins. J. Biol. Chem. *281*, 1612–1619.

58. Rubinstein, M.P., Kovar, M., Purton, J.F., Cho, J.H., Boyman, O., Surh, C.D., and Sprent, J. (2006). Converting IL-15 to a superagonist by binding to soluble IL-15Ralpha. Proc. Natl. Acad. Sci. USA *103*, 9166–9171.

59. Stoklasek, T.A., Schluns, K.S., and Lefrançois, L. (2006). Combined IL-15/IL-15Ralpha immunotherapy maximizes IL-15 activity in vivo. J. Immunol. *177*, 6072–6080.

60. van Meerten, T., van Rijn, R.S., Hol, S., Hagenbeek, A., and Ebeling, S.B. (2006). Complement-induced cell death by rituximab depends on CD20 expression level and acts complementary to antibody-dependent cellular cytotoxicity. Clin. Cancer Res. *12*, 4027–4035.

61. Brudno, J.N., Maric, I., Hartman, S.D., Rose, J.J., Wang, M., Lam, N., Stetler-Stevenson, M., Salem, D., Yuan, C., Pavletic, S., et al. (2018). T cells genetically modified to express an anti-B-cell maturation antigen chimeric antigen receptor cause remissions of poor-prognosis relapsed multiple myeloma. J. Clin. Oncol. *36*, 2267–2280.

YMTHE, Volume *27*

Supplemental Information

Preclinical Evaluation of Allogeneic CAR T Cells Targeting BCMA for the Treatment of Multiple Myeloma

Cesar Sommer, Bijan Boldajipour, Tracy C. Kuo, Trevor Bentley, Janette Sutton, Amy Chen, Tao Geng, Holly Dong, Roman Galetto, Julien Valton, Thomas Pertel, Alexandre Juillerat, Annabelle Gariboldi, Edward Pascua, Colleen Brown, Sherman M. Chin, Tao Sai, Yajin Ni, Philippe Duchateau, Julianne Smith, Arvind Rajpal, Thomas Van Blarcom, Javier Chaparro-Riggers, and Barbra J. Sasu

SUPPEMENTAL INFORMATION

Supplemental Figures

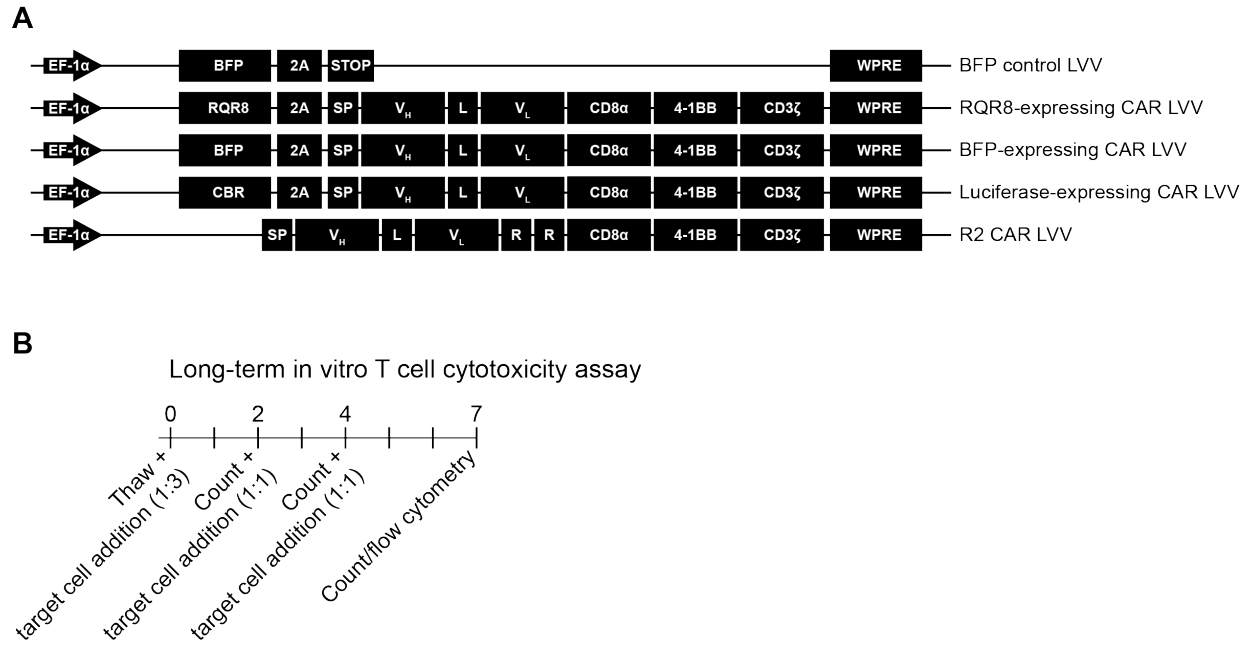

Figure S1. Constructs and experimental outlines. (A) Schematic representation of the lentiviral backbone coding for control or BCMA CAR under control of the human EF-1α promoter. SP: signal peptide, V_H: scFv heavy chain, V_L: scFv light chain: L: GS linker, R: rituximab mimotope flanked by GS linker, 2A: self-cleaving peptide, RQR8: rituximab/ QBEND10-binding fusion protein, CBR: click-beetle red luciferase, BFP: blue-fluorescent protein, WPRE: Woodchuck hepatitis virus post-transcriptional regulatory element. (B) Schematic representation of the long-term cytotoxicity assay after recovery of CAR T from cryopreservation.

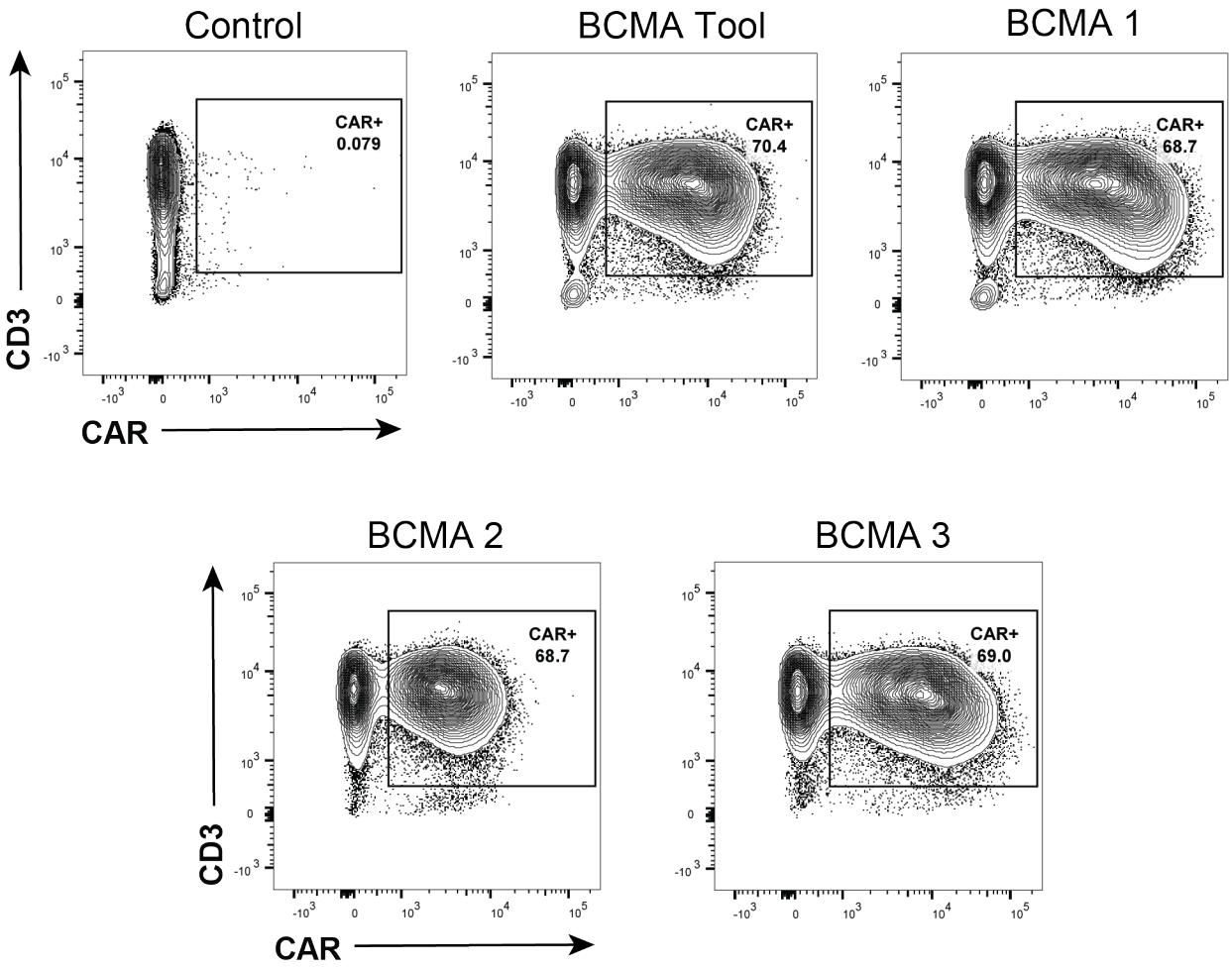

Figure S2. Flow cytometry analysis of CAR expression in BCMA CAR T. Activated T cells were transduced with lentiviral vectors encoding the BCMA CARs and CAR expression was detected by staining with biotinylated-soluble BCMA followed by PE-streptavidin. FACS plots from a donor with high transduction efficiencies are shown.

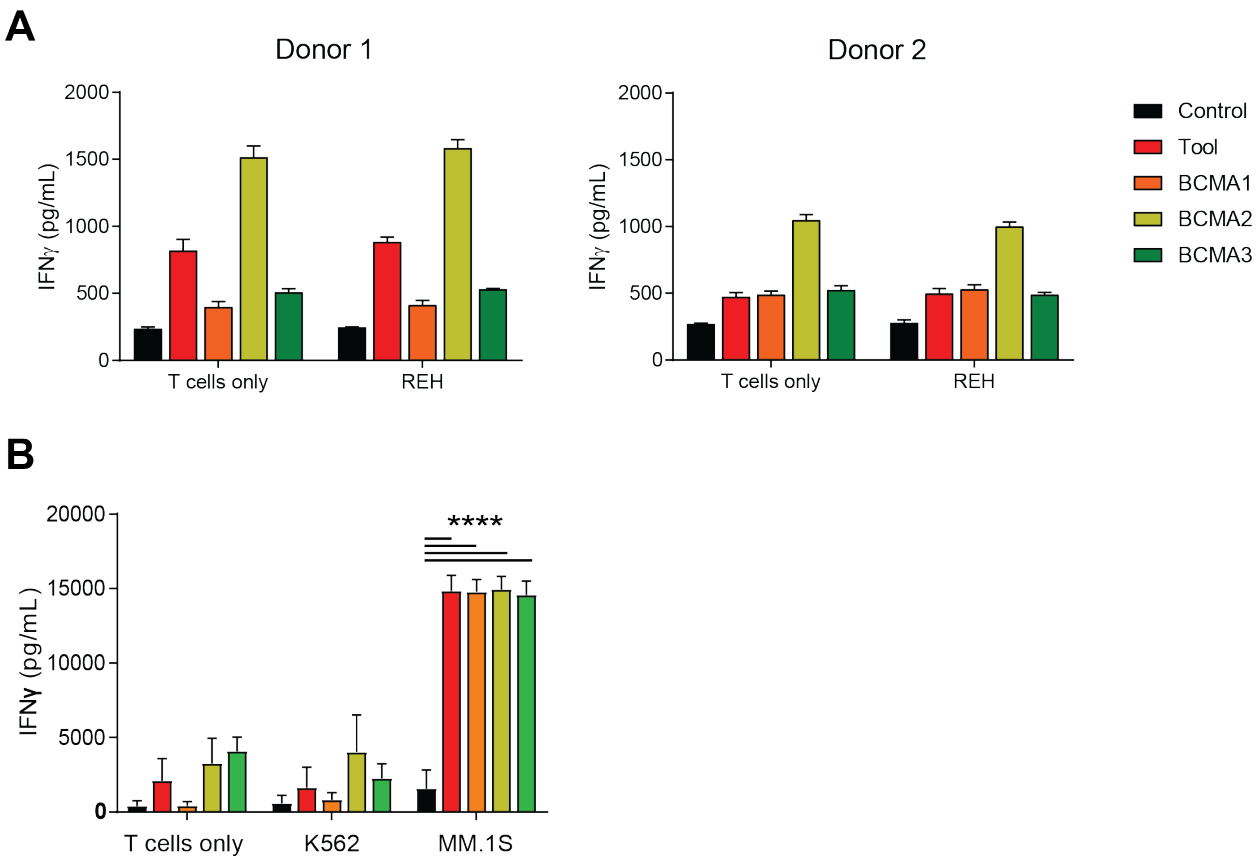

Figure S3. BCMA CAR T exhibit no changes in INFγ secretion when exposed to BCMA-negative cells. (A) IFNγ concentrations were measured on cryopreserved supernatants of BCMA CAR T cultured for 24 hours either alone or with an equal number of BCMA-negative REH cells using ELISA. (B) IFNγ concentrations were measured on cryopreserved supernatants of BCMA CAR T cultured for 24 hours either alone, with BCMA-negative K562 cells, or with BCMA-expressing MM.1S cells, n=4 donors, E:T = 1:1. Data were analyzed using Tukey's one-way ANOVA and all results are shown as mean ± SEM, ****p<0.0001.

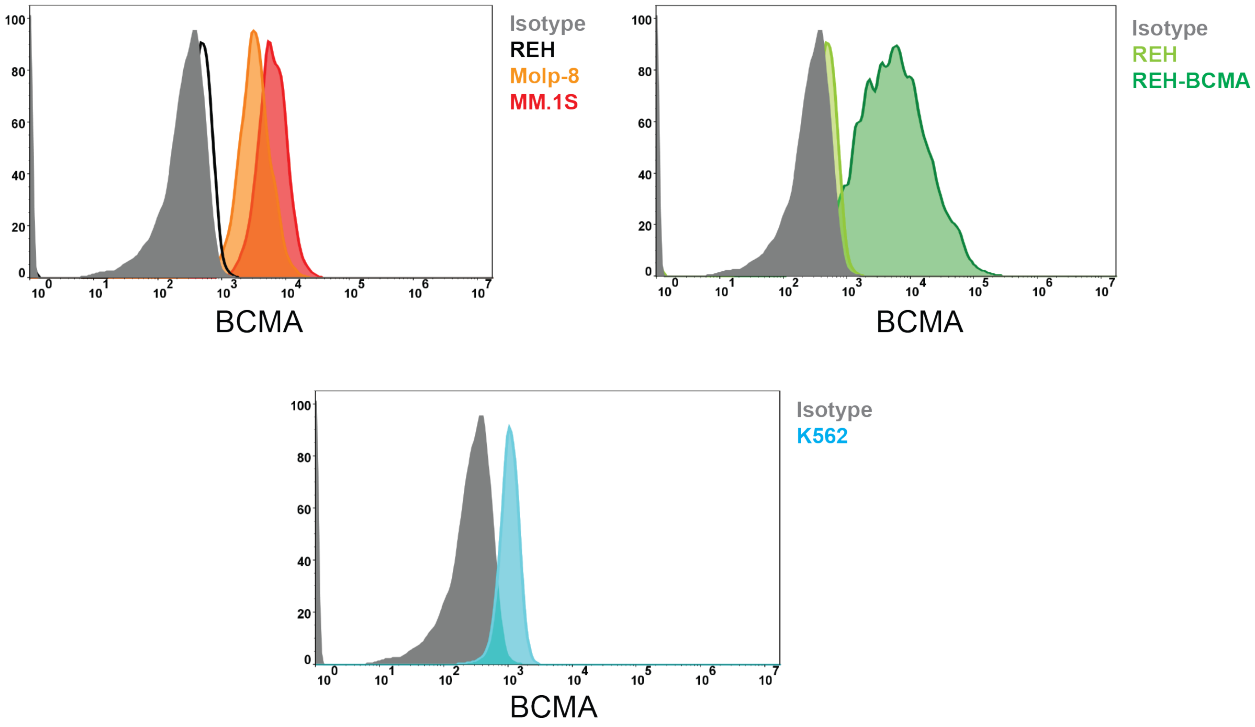

Figure S4. Surface expression of BCMA in target and control cell lines. The surface expression of human BCMA in multiple myeloma (MM.1S, Molp-8) and control cell lines (K562, REH), and in REH cells overexpressing BCMA was assessed by flow cytometry.

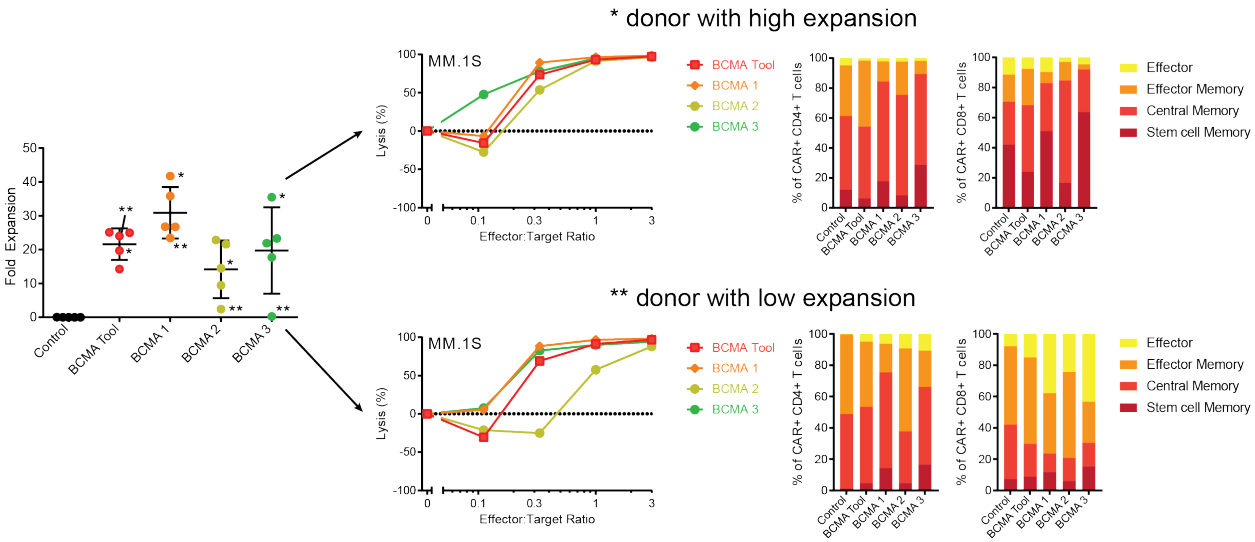

Figure S5. Differences in T cell phenotype affect target-dependent BCMA CAR T expansion and activity. CAR T were stained for CD45RO and CD62L 14 days after expansion and before cryopreservation and analyzed using flow cytometry. CAR T were thawed and expanded on BCMA-expressing target cells for 3 rounds in 7 days, and CAR T expansion was measured using flow cytometry. Expanded CAR T were then cultured with luciferase-expressing MM.1S target cells for 24 hours and cytotoxicity was assessed using bioluminescence readers. Two individual donor products with low and high expansion profiles and their correlating cytotoxicity and phenotype profiles are shown.

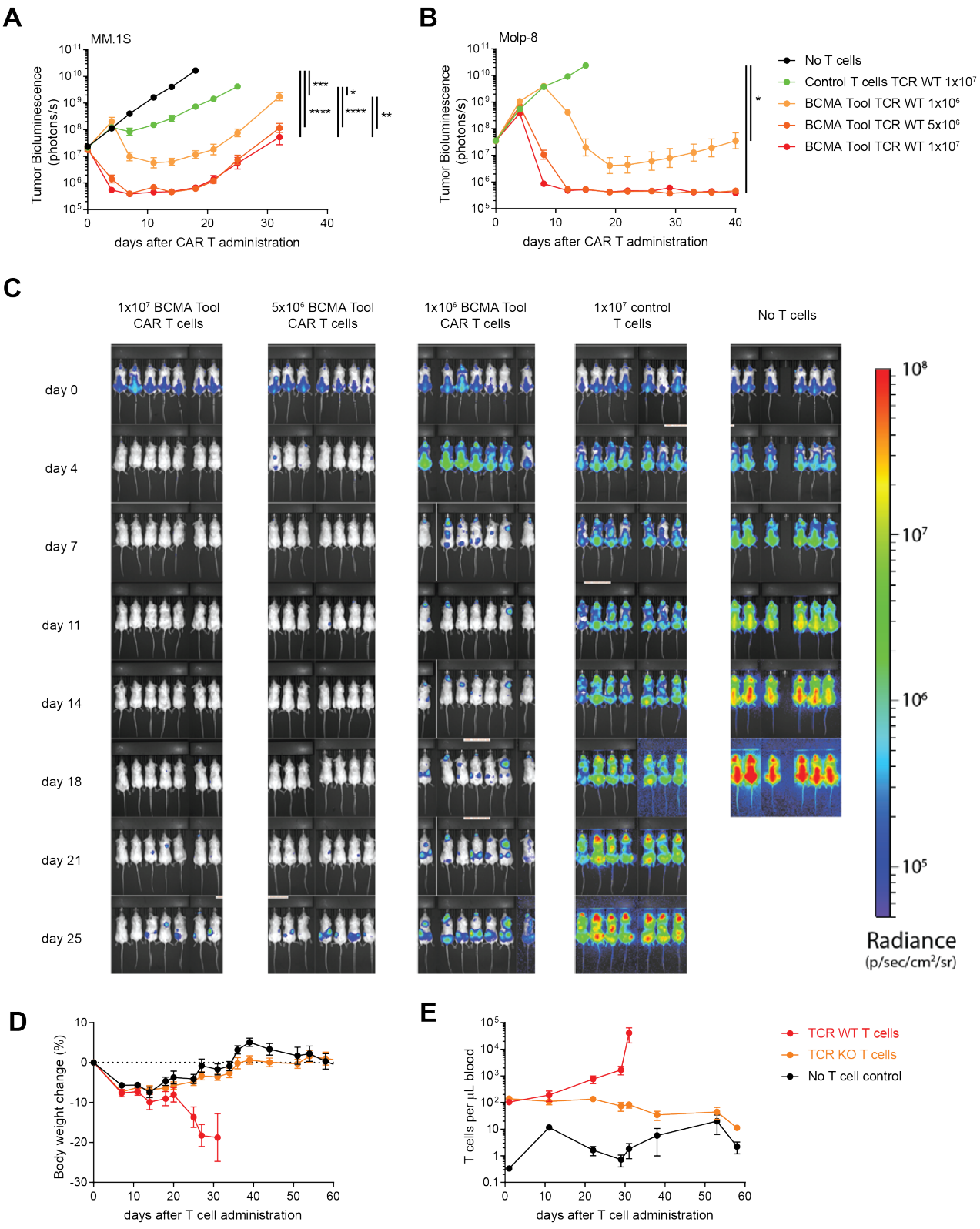

Figure S6. Development of animal models to test BCMA CAR T activity. (A-B) BCMA tool CAR T showed potent efficacy in two orthotopic tumor models. NSG mice were injected with luciferase-expressing MM.1S (A) or Molp-8 cells (B). Tumor-bearing mice received the indicated dose of CAR$^+$ cells together with control T cells to

match the total number of T cells across all groups (total of $1.3x10^7$ cells). Tumor growth was assessed using whole-body luminescence imaging. n=7 in (A), n=10 in (B). (C) Tumor-bearing mice treated with BCMA CAR T relapse with discrete tumors outside of the bone marrow. Bioluminescence images of mice in (A). (D-E) Gene-edited BCMA CAR T did not cause GvHD in a xenogeneic model. (D) NSG mice received 2 Gy total body irradiation and $3x10^7$ T cells ($1.8\text{-}2.0x10^7$ CAR^+ cells) and body weight was measured as readout for GvH responses. n=10 animals. (E) Peripheral blood cells of mice in (D) were stained using CD45 antibodies and quantified using flow cytometry. A-B were analyzed using Tukey's repeated measures one-way ANOVA. All results are shown as mean ± SEM. Asterisks show statistical significance against the indicated condition. *p<0.05, **p<0.01, ***p<0.001, ****p<0.0001.

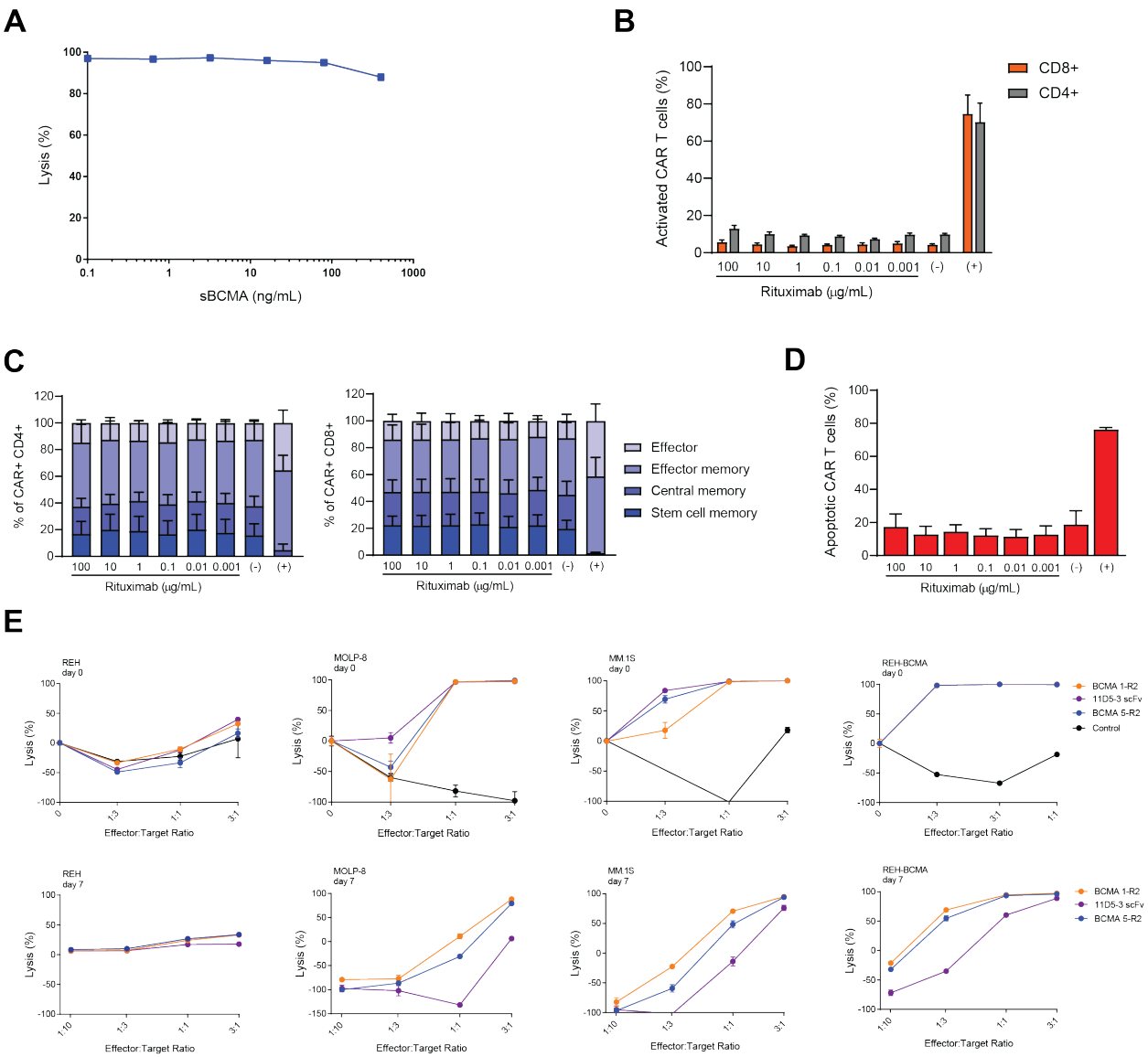

Figure S7. Effects of soluble BCMA (sBCMA) and rituximab on BCMA CAR T and comparison with 11D5-3 anti-BCMA CAR. (A) BCMA 1-R2 CAR T were cultured with luciferase-expressing MM.1S cells in the presence of increasing concentrations of sBCMA (up to 400 ng/mL) and residual target cell viability was determined at 24 hours by luminescence analysis. (B-C) Rituximab does not influence BCMA 1-R2 CAR T activation or differentiation, as evaluated by flow cytometry analysis of the expression of 4-1BB (B) and the differentiation markers CD62L and CD45RO (C) on CAR T cultured with increasing concentrations of the antibody for 24 hours. CAR T stimulated with PMA/ionomycin served as positive control (n=3 donors). (D) Rituximab does not influence the apoptotic rate of BCMA 1-R2 CAR T, as determined by flow cytometry analysis of CAR T cultured with increasing concentrations of the antibody for 24 hours using Annexin V protein conjugated with FITC. CAR T stimulated with PMA/ionomycin served as positive control (n=3 donors). (E) Comparable activity of BCMA 1-R2, BCMA 5-R2 and 11D5-3 CAR T. The 11D5-3 CAR consists of the 11D5-3 scFv followed by a CD8 hinge/TM region and 4-1BB and CD3ζ signaling domains. CAR T were cultured with luciferase-expressing target cell lines or a BCMA-negative control cell line and residual luciferase activity was measured at 24 hours (*Top panel*). The activities of the three CARs were also evaluated after seven days of continuous exposure to target (*Bottom panel*).

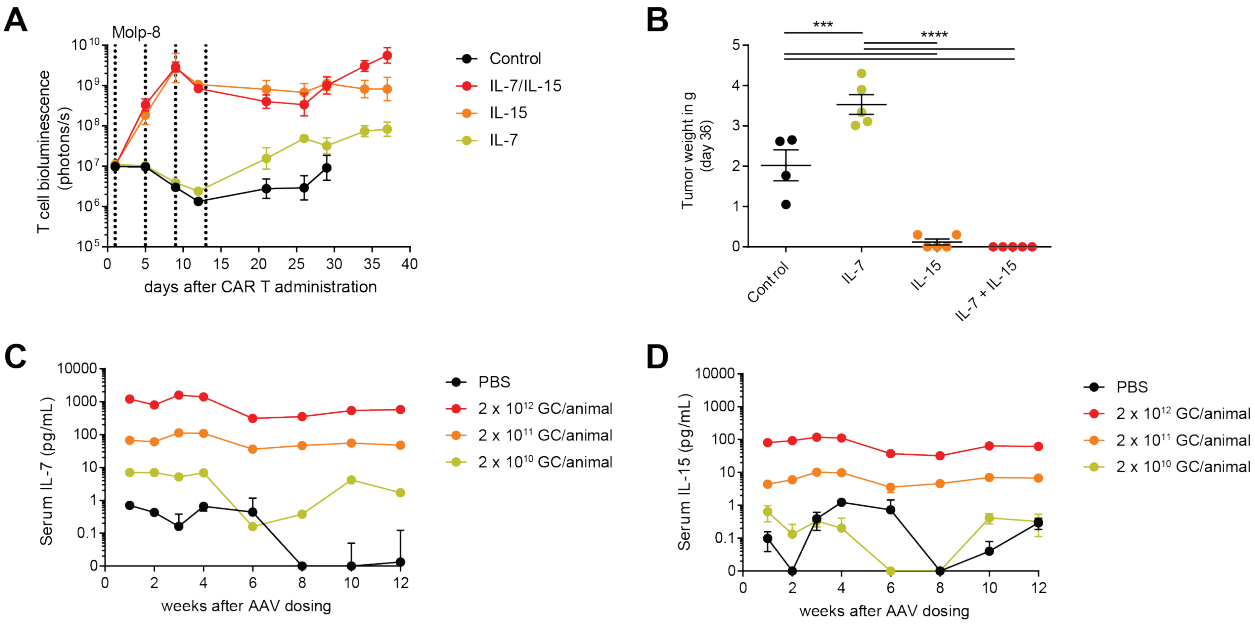

Figure S8. Exogenous homeostatic cytokines support expansion of BCMA CAR T in NSG mice. (A-B) Exogenous IL-15 enhanced proliferation and activity of BCMA Tool CAR T in an orthotopic Molp-8 model. (A) NSG mice were injected with Molp-8 cells and $1x10^6$ click-beetle red luciferase-expressing BCMA Tool CAR T (total of $8.3x10^6$ T cells) 8 days later. 500 ng of human recombinant IL-7 and IL-15 were complexed in vitro with equimolar amounts of either IL-7 or IL-15Rα-Fc for 30 minutes before i.p. administration to mice as indicated by dotted lines. CAR T expansion and persistence were assessed using whole-body luminescence imaging. n=5 mice per group. (B) Total tumor mass of animals in (A) was determined during necropsy on day 36 after CAR T administration. Visible tumors were collected from all body parts except the brain. n=4-5 animals, Tukey's one-way ANOVA. (C-D) Mice injected with AAV9 pseudotyped viruses coding for human IL-7 or IL-15/IL-15Rα fusion proteins stably express human cytokines at near physiological levels. Viruses were injected at the indicated titers (genomic contents per animal) into the tail vein of NSG mice and the cytokine concentration in peripheral blood was determined using ELISA. n=3 animals.

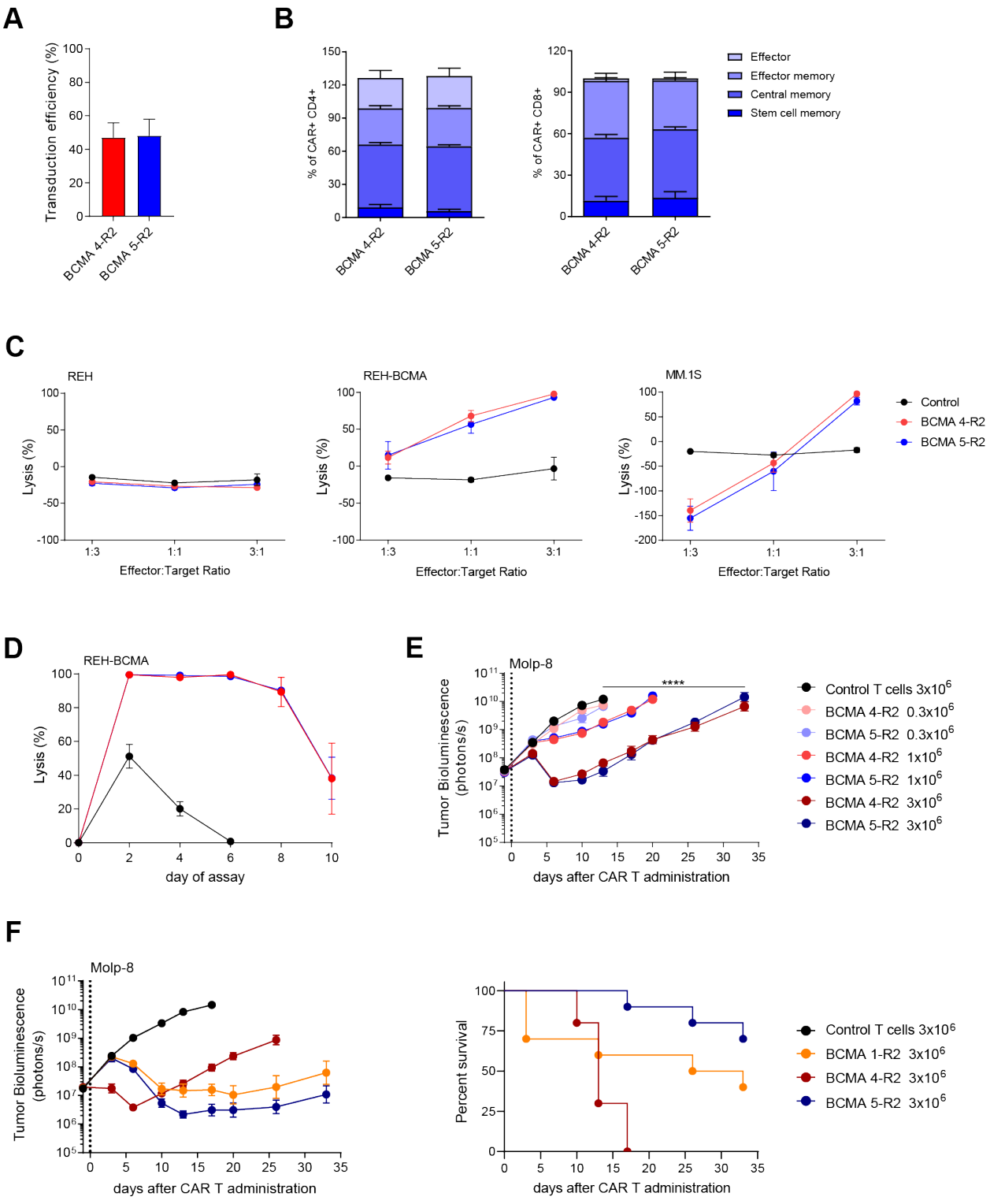

Figure S9. Two additional BCMA CAR T candidates have equivalent activity in vitro and in vivo. (A) Both BCMA CAR T candidates demonstrated similar transduction efficiencies as detected by soluble BCMA staining or BFP expression via flow cytometry at day 16 of expansion. n=5 donors. (B) BCMA CAR T candidates showed similar differentiation phenotypes. CAR T were analyzed using flow cytometry 16 days after activation and phenotypes were assigned according to CD62L and CD45RO expression within the CAR^+ population. n=5 donors.

(C) BCMA CAR T candidates showed similar cytotoxicity against BCMA-expressing target cells. CAR T were cultured with luciferase-expressing BCMA-negative REH cells, REH cells overexpressing BCMA, or the MM cell line MM.1S. Target cell luminescence was assessed after 24 hours. n=5 donors. (D) Candidates maintained cytotoxicity after repeated exposure to target cells. $1x10^6$ BCMA CAR T were mixed with $1x10^6$ GFP-expressing REH-BCMA cells and incubated for 48 hours. 5% of the culture was removed and GFP^+ tumor cells were quantified using flow cytometry. $1x10^6$ REH-BCMA cells were added to the culture and the assay was repeated for a total of 5 times. n=4 donors. (E) BCMA CAR T candidates performed similarly in an orthotopic Molp-8 tumor model. Tumor-bearing animals received TCR-wild type CAR^+ cells at the indicated doses in a total of $6.9x10^6$ cells. Tumor growth was assessed using whole-body luminescence imaging (n=10). (F) BCMA 4-R2 and BCMA 5-R2 were tested against BCMA 1-R2 CAR T in an orthotopic Molp-8 tumor model as in (E). n=8-10. A-C were analyzed using Tukey's one-way ANOVA. E and F were analyzed using Tukey's repeated-measures one-way ANOVA. All results are shown as mean ± SEM. Asterisks show statistical significance against the indicated condition, *$p<0.05$, **$p<0.01$, ***$p<0.001$, ****$p<0.0001$.

Table S1. Binding affinities of anti-BCMA antibodies

Antibody	K_D (nM)
BCMA 1	0.19 nM
BCMA 2	0.54 nM
BCMA 3	0.04 nM
BCMA 4	0.038 nM
BCMA 5	5.57 nM

The affinities of the anti-BCMA antibodies for human BCMA were determined at 37°C by surface plasmon resonance. K_D = equilibrium dissociation constant.

Supplemental Methods

Cells and culture conditions

Cell lines and primary cells were cultured in a humidified incubator at 37ºC and 5% CO_2. The cell lines HEK293T (CRL-3216), K562 (CCL-243), MM.1S (CRL-2974), and REH (CRL-8286) were acquired from ATCC (Manassas, VA). Molp-8 cells (ACC-569) were obtained from Deutsche Sammlung von Mikroorganismen und Zellkulturen (DSMZ, Braunschweig, Germany). Tumor cell lines were engineered to express Luciferase and GFP using Luc2AGFP lentivirus (AMSbio, Cambridge, MA). Peripheral blood mononuclear cells (PBMC) were sourced from Stanford Blood Center (Palo Alto, CA) or Stemcell Technologies (Vancouver, BC, Canada) and T cells were isolated using the human Pan T Cell Isolation Kit (Miltenyi Biotec, Auburn, CA).

Protein Reagents

The extracellular domain of the human BCMA protein (NM_001192.2) fused to a C-terminal 10x His Tag and Avi Tag was expressed in Expi293 cells and purified from culture supernatants. The recombinant protein was biotinylated using the Bulk BirA ligase reaction kit (Avidity, Aurora, CO). Rituximab and alemtuzumab sequences were obtained from public sources. An anti-idiotype antibody against the BCMA 1 scFv was raised in Balb/c mice and was purified from hybridoma cell culture supernatants. Antibodies were labeled with R-PE (Prozyme, Hayward, CA) using sulfhydryl-maleimide reaction chemistry.

Lentiviral vector production

HEK293T cells were transfected with lentiviral transfer vectors, psPAX2, and pMD.2G (École Polytechnique Fédérale de Lausanne, France) using Lipofectamine 2000 (Thermo Fisher Scientific, Waltham, MA). Twenty-four hours after transfection, the medium was replaced with X-Vivo 15 medium (Lonza, Basel, Switzerland) supplemented with 10% FCS (GE Healthcare, Pittsburgh, PA). Virus-containing supernatants were harvested 24 hours later.

Production of allogeneic CAR T

T cells were isolated from healthy donor PBMC using T cell negative selection kits (Miltenyi Biotec, Auburn, CA Biotec) and cryopreserved in FCS/10% DMSO. Immediately after thawing, T cells were cultured in X-Vivo 15 medium (Lonza) supplemented with 10% FCS (GE Healthcare, Pittsburgh, PA) and 20 ng/mL IL-2 (Miltenyi Biotec, Auburn, CA) and activated using T cell TransAct™ (Miltenyi Biotec, Auburn, CA). 2 days after activation, T cells were transduced for 24 hours, then resuspended in X-Vivo 15 medium supplemented with 5% human AB serum (Gemini Bio-Products, West Sacramento, CA). IL-2 was supplemented every 2 days. Plasmids encoding TALEN® monomers for TRAC and CD52 were obtained from Cellectis, Paris, France (Poirot et al, 2015) and used for TALEN® mRNA synthesis (TriLink Biotechnologies, San Diego, CA). 7 days after activation, T cells were electroporated with 25 μg/mL per TALEN® mRNA using AgilePulse MAX electroporators (BTX, Holliston, MA). T cells were cultured in X-Vivo 15 medium with 5% human serum and 20 ng/mL IL-2 at 30ºC for 24 hours before continuing expansion at 37ºC. 17 days after activation, depletion of $TCR\alpha^+$ cells was performed using CliniMACS TCRαβ kits (Miltenyi Biotec, Auburn, CA), followed by recovery in X-Vivo 15 medium supplemented with 5% human serum and 20 ng/mL IL-2. 18 days after activation, T cells were cryopreserved in 90% FCS/10% DMSO using rate-controlled freezing chambers and stored in liquid nitrogen vapor phase. For large-scale production, the same protocol was followed with adaptations: Healthy-donor PBMC (Hemacare, Los Angeles, CA) were thawed and activated 24 hours later with T cell Transact™ (Miltenyi Biotec, Auburn, CA) and IL-2. 3 days after activation, T cells were transduced with concentrated lentiviral vector (Miltenyi Biotec, Auburn, CA) and electroporated with TALEN® mRNA 48 hours later. 7 days after activation, cells were expanded in 2L WAVE bag bioreactors (GE Healthcare, Pittsburgh, PA). Depletion of $TCR\alpha^+$ cells was performed 17 days after activation and T cells were frozen 18 days after activation in CS5 cryoprotectant (Stemcell Technologies, Vancouver, BC, Canada). A schematic of T cell culture timelines is given in Figure 6A. All functional assays were performed with cells after recovery from cryopreservation.

Determination of the binding affinities of anti-BCMA antibodies to human BCMA

Surface Plasmon Resonance (SPR) experiments were performed as follows. An anti-human IgG Fc capture chip was prepared by amine-coupling of goat anti-human IgG Fc (Southern Biotech, Birmingham, AL) to a Biacore Series S sensor chip CM4 (GE Lifesciences, Marlborough, MA) surface at 25°C. Kinetic assays were conducted at 37°C in running buffer HBST+ supplemented with 1 mg/mL bovine serum albumin. IgG-containing cell culture supernatants were injected for 2 minutes at 10 µL/min onto a downstream flowcell (resulting in different IgGs being immobilized in flowcell 2, 3 or 4). In all experiments, flowcell 1 was used as a reference surface. Human BCMA was diluted into running buffer at concentrations of 5 and 25 nM, injected as analyte for two minutes at 30 µL/min and dissociation was monitored for 20 minutes. The anti-human IgG Fc surfaces were regenerated using three 60-second injections of 75 mM phosphoric acid between each analyte binding cycle. All sensorgrams were double-referenced and fit to a 1:1 Langmuir binding with mass transport model using Biacore T200 Evaluation Software (Version 2.0).

References

Poirot L, Philip B, Schiffer-Mannioui C, et al. Multiplex Genome-Edited T-cell Manufacturing Platform for "Off-the-Shelf" Adoptive T-cell Immunotherapies. Cancer research. 2015;75(18):3853-3864.